



*Pavia  
University*

*Phys. Dept.  
"A. Volta"*



# The Guided-Mode Expansion Method for Photonic Crystal Slabs

Lucio Claudio Andreani

*Dipartimento di Fisica "Alessandro Volta,"  
Università degli Studi di Pavia, via Bassi 6, 27100 Pavia, Italy*

[andreani@fiscavolta.unipv.it](mailto:andreani@fiscavolta.unipv.it)  
<http://fiscavolta.unipv.it/dipartimento/ricerca/fotonici/>

***COST P11 Training School, Univ. of Nottingham, June 19-22, 2006***

## Acknowledgements

### ***Collaboration:***

**Mario Agio** (now at Physical Chemistry Laboratory, ETH-Zurich)

**Dario Gerace** (now at Institute of Quantum Electronics, ETH Zurich)

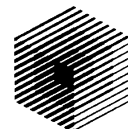
### ***Support:***

**MIUR** (Italian Ministry for Education, University and Research) under Cofin program "Silicon-based photonic crystals" and FIRB project "Miniaturized electronic and photonic systems"

**INFN** (National Institute for the Physics of Matter) under PRA (Advanced Research Project) "PHOTONIC"



*Ministero dell'Istruzione  
dell'Università e Ricerca*



**Fisica della Materia**

# Outline

## 1. Required notions

- Basic properties of photonic band structure
- Plane-wave expansion
- Dielectric slab waveguide
- Waveguide-embedded photonic crystals

## 2. Guided-mode expansion method

- Photonic mode dispersion
- Intrinsic diffraction losses
- Convergence tests, comparison with other methods
- Examples of applications

Photonic crystals are materials in which the dielectric constant is periodic in 1D, 2D or 3D...

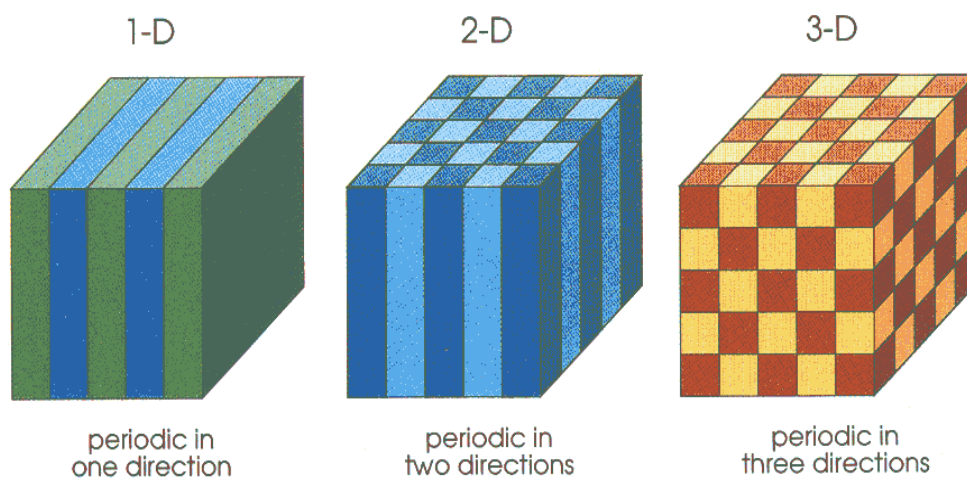


**Figure 1** Simple examples of one-, two-, and three-dimensional photonic crystals. The different colors represent materials with different dielectric constants. The defining feature of a photonic crystal is the periodicity of dielectric material along one or more axes.

... leading to the formation of photonic bands and gaps.

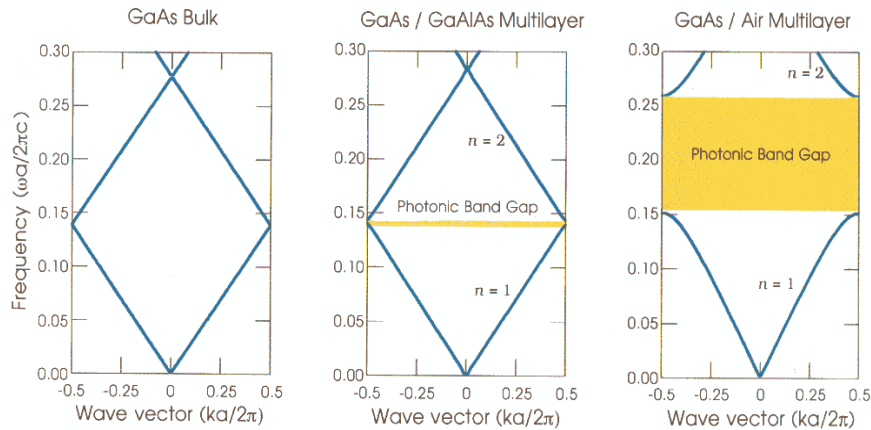


**Figure 2** The photonic band structures for on-axis propagation, shown for three different multilayer films, all of which have layers of width  $0.5a$ . *Left*: each layer has the same dielectric constant  $\epsilon = 13$ . *Center*: layers alternate between  $\epsilon = 13$  and  $\epsilon = 12$ . *Right*: layers alternate between  $\epsilon = 13$  and  $\epsilon = 1$ .

A full photonic band gap in 3D may allow to achieve

- suppression of spontaneous emission (*E. Yablonovitch, 1987*)
- localization of light by disorder (*S. John, 1987*)

## Books:

Joannopoulos JD, Meade RD and Winn JN, *Photonic Crystals – Molding the Flow of Light* (Princeton University Press, Princeton, 1995).

Johnson SG and Joannopoulos JD, *Photonic Crystals: the Road from Theory to Practice* (Kluwer Academic Publishers, Boston, 2001).

Sakoda K: *Optical Properties of Photonic Crystals*, Springer Series in Optical Sciences, Vol. **80**. (Springer, Berlin, 2001).

Busch K, Lölkes S, Wehrspohn RB, Föll H: *Photonic Crystals – Advances in Design, Fabrication and Characterization* (Wiley-VCH, Weinheim, 2004).

Lourtioz JM, Benisty H, Berger V, Gérard JM, Maystre D, Tchebnokov A: *Photonic Crystals: Towards Nanoscale Photonic Devices* (Springer, Berlin, 2005).

# Maxwell equations in matter

no sources, unit magnetic permeability

First-order, time-dependent:

$$\nabla \times \mathbf{E} = -\frac{1}{c} \frac{\partial \mathbf{B}}{\partial t}$$

$$\nabla \times \mathbf{H} = \frac{1}{c} \frac{\partial \mathbf{D}}{\partial t}$$

$$\nabla \cdot \mathbf{D} = 0$$

$$\nabla \cdot \mathbf{B} = 0$$

$$\mathbf{D}(\mathbf{r}) = \varepsilon(\mathbf{r})\mathbf{E}(\mathbf{r})$$

$$\mathbf{H}(\mathbf{r}) = \mathbf{B}(\mathbf{r})$$

Second-order, harmonic time dependence  $\psi(t) = \psi e^{-i\omega t}$  :

$$\nabla \times \nabla \times \mathbf{E}(\mathbf{r}) = \frac{\omega^2}{c^2} \varepsilon(\mathbf{r}) \mathbf{E}(\mathbf{r})$$

$$\nabla \cdot [\varepsilon(\mathbf{r}) \mathbf{E}(\mathbf{r})] = 0$$

$$\mathbf{H}(\mathbf{r}) = -i \frac{c}{\omega} \nabla \times \mathbf{E}(\mathbf{r})$$

$$\nabla \times \left[ \frac{1}{\varepsilon(\mathbf{r})} \nabla \times \mathbf{H}(\mathbf{r}) \right] = \frac{\omega^2}{c^2} \mathbf{H}(\mathbf{r})$$

$$\nabla \cdot \mathbf{H}(\mathbf{r}) = 0$$

$$\mathbf{E}(\mathbf{r}) = i \frac{c}{\omega} \frac{1}{\varepsilon(\mathbf{r})} \nabla \times \mathbf{H}(\mathbf{r})$$

## Translational invariance

If the photonic lattice is invariant under translations by the vectors  $\mathbf{R}$  of a Bravais lattice,

$$\varepsilon(\mathbf{r} + \mathbf{R}) = \varepsilon(\mathbf{r}),$$

then Bloch-Floquet theorem holds for any component of the fields:

$$\psi_{n\mathbf{k}}(\mathbf{r}) = e^{i\mathbf{k} \cdot \mathbf{r}} u_{n\mathbf{k}}(\mathbf{r}), \quad u_{n\mathbf{k}}(\mathbf{r} + \mathbf{R}) = u_{n\mathbf{k}}(\mathbf{r})$$

The frequencies are grouped into *photonic bands*:

$$\omega = \omega_n(\mathbf{k})$$

N.b. the system is assumed to be *infinitely extended* along the directions of periodicity  $\rightarrow$  the Bloch vector  $\mathbf{k}$  is *real*.

It is usually chosen to lie in the first Brillouin zone (*band folding*).

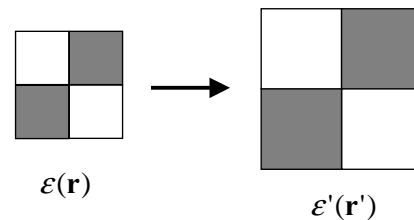
# Eigenvalue problem & scale invariance

$$\nabla \times \left[ \frac{1}{\varepsilon(\mathbf{r})} \nabla \times \mathbf{H}(\mathbf{r}) \right] = \frac{\omega^2}{c^2} \mathbf{H}(\mathbf{r}) \quad \left\{ \begin{array}{l} \hat{\Theta} \mathbf{H}(\mathbf{r}) = \lambda \mathbf{H}, \quad \lambda = \frac{\omega^2}{c^2} \\ \hat{\Theta} = \nabla \times \frac{1}{\varepsilon(\mathbf{r})} \nabla \times \end{array} \right. \quad \text{Hermitian operator}$$

Hermitian eigenvalue problem (*like for electron states in quantum mechanism*)

$$\mathbf{r} \rightarrow \mathbf{r}' = s\mathbf{r}, \quad \varepsilon'(\mathbf{r}') = \varepsilon(\mathbf{r})$$

$$\Rightarrow \omega_n'(\mathbf{k}') = \frac{\omega_n(\mathbf{k})}{s}$$



Scale invariance: photonic band structure is unique when expressed in dimensionless units  $\omega a / (2\pi c)$  versus  $ka$  ( $a$ =lattice constant)

## 1. Required notions

- Basic properties of photonic band structure
- Plane-wave expansion
- Dielectric slab waveguide
- Waveguide-embedded photonic crystals

## 2. Guided-mode expansion method

- Photonic mode dispersion
- Intrinsic diffraction losses
- Convergence tests, comparison with other methods
- Examples of applications

# Plane-wave expansion in 3D

Expansion of the magnetic field in plane waves with reciprocal lattice vectors  $\mathbf{G}$ :

$$\mathbf{H}_{n\mathbf{k}}(\mathbf{r}) = \sum_{\mathbf{G}, \lambda} c_n(\mathbf{k} + \mathbf{G}, \lambda) \hat{\mathbf{e}}(\mathbf{k} + \mathbf{G}, \lambda) e^{i(\mathbf{k} + \mathbf{G}) \cdot \mathbf{r}}$$

where  $\hat{\mathbf{e}}(\mathbf{k} + \mathbf{G}, \lambda) \equiv \hat{\mathbf{e}}_\lambda, \lambda = 1, 2$  are two orthogonal unit vectors perpendicular to  $\mathbf{k} + \mathbf{G}$ . The second-order equation for  $\mathbf{H}$  becomes:

$$\sum_{\mathbf{G}', \lambda'} H_{\mathbf{k} + \mathbf{G}, \lambda; \mathbf{k} + \mathbf{G}', \lambda'} c_n(\mathbf{k} + \mathbf{G}', \lambda') = \frac{\omega^2}{c^2} c_n(\mathbf{k} + \mathbf{G}, \lambda)$$

$$H_{\mathbf{k} + \mathbf{G}, \lambda; \mathbf{k} + \mathbf{G}', \lambda'} = |\mathbf{k} + \mathbf{G}| |\mathbf{k} + \mathbf{G}'| \epsilon^{-1}(\mathbf{G}, \mathbf{G}') \begin{bmatrix} \hat{\mathbf{e}}_2 \cdot \hat{\mathbf{e}}_2' & -\hat{\mathbf{e}}_2 \cdot \hat{\mathbf{e}}_1' \\ -\hat{\mathbf{e}}_1 \cdot \hat{\mathbf{e}}_2' & \hat{\mathbf{e}}_1 \cdot \hat{\mathbf{e}}_1' \end{bmatrix}$$

with the inverse dielectric matrix being defined as ( $v$ =unit cell volume)

$$\epsilon^{-1}(\mathbf{G}, \mathbf{G}') = \frac{1}{v} \int \epsilon^{-1}(\mathbf{r}) e^{i(\mathbf{G}' - \mathbf{G}) \cdot \mathbf{r}} d\mathbf{r},$$

## Choice of plane waves

The infinite sum over  $\mathbf{G}$  is truncated to a finite number  $N$  of reciprocal lattice vectors, usually chosen by introducing a wavevector cutoff:

$$|\mathbf{G}| < \Lambda$$

The dimension of the linear eigenvalue problem is  $(2N) \times (2N)$ . The matrix  $H$  is

- \* *real symmetric* if  $\epsilon(\mathbf{r})$  has a center of inversion (taken to be the origin)
- \* *complex hermitian* if  $\epsilon(\mathbf{r})$  has no center of inversion

N.b. The cut-off condition restricts the numbers  $N$  to be used: e.g., for the fcc lattice,  $N=1, 9, 15, \dots$ . If other values of  $N$  are chosen, unphysical splittings at  $\mathbf{k}=0$  may arise

# Direct and inverse dielectric matrix

$$\varepsilon(\mathbf{G}, \mathbf{G}') = \frac{1}{v} \int \varepsilon(\mathbf{r}) e^{i(\mathbf{G}' - \mathbf{G}) \cdot \mathbf{r}} d\mathbf{r} \quad (1)$$

$$\varepsilon^{-1}(\mathbf{G}, \mathbf{G}') = \frac{1}{v} \int \varepsilon^{-1}(\mathbf{r}) e^{i(\mathbf{G}' - \mathbf{G}) \cdot \mathbf{r}} d\mathbf{r} \quad (2)$$

In the limit  $N \rightarrow \infty$ , it is equivalent to evaluate  $\varepsilon^{-1}(\mathbf{G}, \mathbf{G}')$  from (2) or as a numerical inversion of the direct dielectric matrix (1):

$$\varepsilon^{-1}(\mathbf{G}, \mathbf{G}') = [\varepsilon(\mathbf{G}, \mathbf{G}')]^{-1} \quad \text{Ho, Chan and Soukoulis, PRL 65, 3152 (1990)}$$

However, the two procedures have different convergence properties for finite  $N$ .

The procedure by Ho, Chan and Soukoulis generally yields much faster convergence as a function of  $N$ .

## Fourier factorization rules

Consider the Fourier transform  $A$  of a product of functions  $B$  and  $C$ :

$$A_G = \sum_{G'=-\infty}^{+\infty} B_{G-G'} C_{G'}$$

When the sum is truncated to a finite number  $N$  of harmonics, the above expression does not converge uniformly if both  $B$  and  $C$  are discontinuous at the same point while  $A=BC$  remains continuous. In this case the inverse rule yields uniform convergence and should be used:

$$A_G = \sum_{G'=-M}^{+M} \left( \frac{1}{B} \right)_{G-G'}^{-1} C_{G'}$$

In the presence of a sharp discontinuity of  $\varepsilon(\mathbf{r})$ , expressions like  $\varepsilon \mathbf{E}$  should be treated according to the direct (inverse) rule when the continuous (discontinuous) component  $E_{\parallel}$  ( $E_{\perp}$ ) of the field is involved.

L.F. Li, JOSA A 13, 1870 (1996); P. Lalanne, PRB 58, 9801 (1998);  
S.G. Johnson and J.D. Joannopoulos, Opt. Expr. 8, 173 (2001);  
A. David et al., PRB 73, 075107 (2006)

# Complete photonic band gap in 3D: the diamond lattice of dielectric spheres

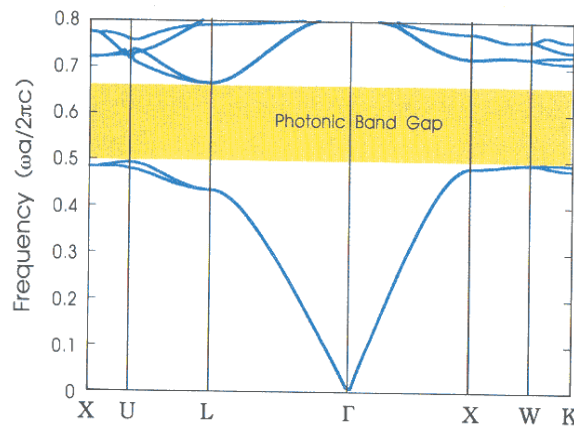


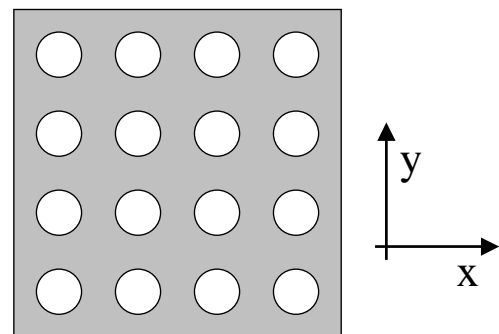
**Figure 3** The photonic band structure for the lowest six bands of a diamond lattice of air spheres in a high dielectric ( $\epsilon = 13$ ) material. The wave vector varies across the irreducible Brillouin zone, from  $\Gamma$  to X to W to K, then back to  $\Gamma$  through X, U, and L. See appendix B for a discussion of the Brillouin zone for a face-centered cubic lattice.

K.M. Ho, C.T. Chan and C.M. Soukoulis, Phys. Rev. Lett. **65**, 3152 (1990)

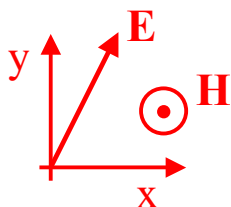
## 2D photonic crystals: parity separation

Specular reflection in the  $xy$  plane is a symmetry operation of the system, which we denote by  $\hat{\sigma}_{xy}$ .

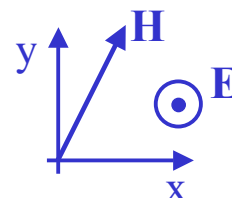
Thus for in-plane propagation we can distinguish



Even,  $\sigma_{xy}=+1$  modes (TE, H modes):  
components  $E_x, E_y, H_z$



Odd,  $\sigma_{xy}=-1$  modes (TM, E modes):  
components  $H_x, H_y, E_z$





# Plane-wave expansion in 2D

The expansion of the field contains 2D vectors  $\mathbf{k}$  and  $\mathbf{G}$ :

$$\mathbf{H}_{n\mathbf{k}}(\mathbf{r}) = \sum_{\mathbf{G}, \lambda} c_n(\mathbf{k} + \mathbf{G}, \lambda) \hat{\mathbf{e}}(\mathbf{k} + \mathbf{G}, \lambda) e^{i(\mathbf{k} + \mathbf{G}) \cdot \mathbf{r}}$$

The polarization vectors can be chosen as:

$$\hat{\mathbf{e}}(\mathbf{k} + \mathbf{G}, 1) \equiv \hat{\mathbf{z}}, \quad \hat{\mathbf{e}}(\mathbf{k} + \mathbf{G}, 2) \equiv \hat{\mathbf{z}} \times \hat{\mathbf{k}}$$

Thus the  $(2N) \times (2N)$  matrix of the eigenvalue problem decouples as:

$$H_{\mathbf{k}+\mathbf{G}, \lambda; \mathbf{k}+\mathbf{G}', \lambda'} = \varepsilon^{-1}(\mathbf{G}, \mathbf{G}') \begin{bmatrix} (\mathbf{k} + \mathbf{G}) \cdot (\mathbf{k} + \mathbf{G}') & 0 \\ 0 & |\mathbf{k} + \mathbf{G}| |\mathbf{k} + \mathbf{G}'| \end{bmatrix}$$

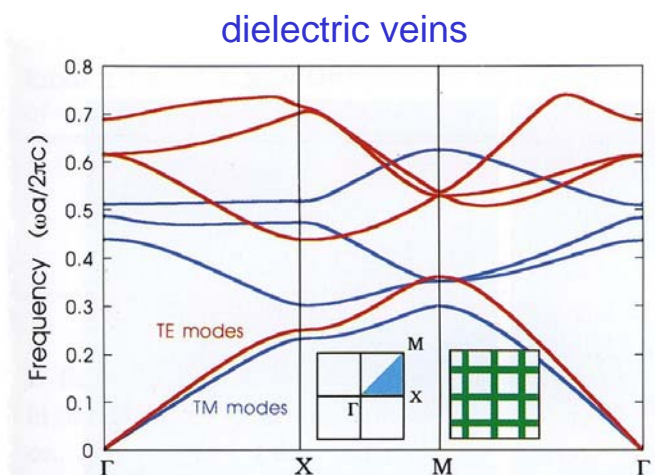
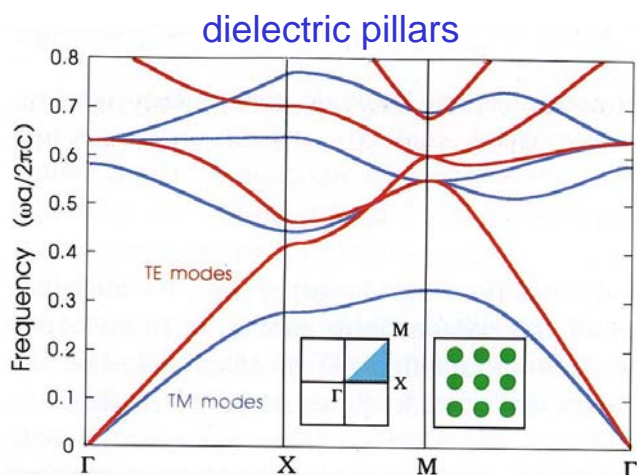
where the upper (lower) block corresponds to H (E) modes.

N.b. off-plane propagation,  $k_z \neq 0$ : no parity separation, 3D PWE

## Polarization-dependent gap in 2D: the square lattice

**TE or H modes:  $H_z, E_x, E_y$**

**TM or E modes:  $E_z, H_x, H_y$**

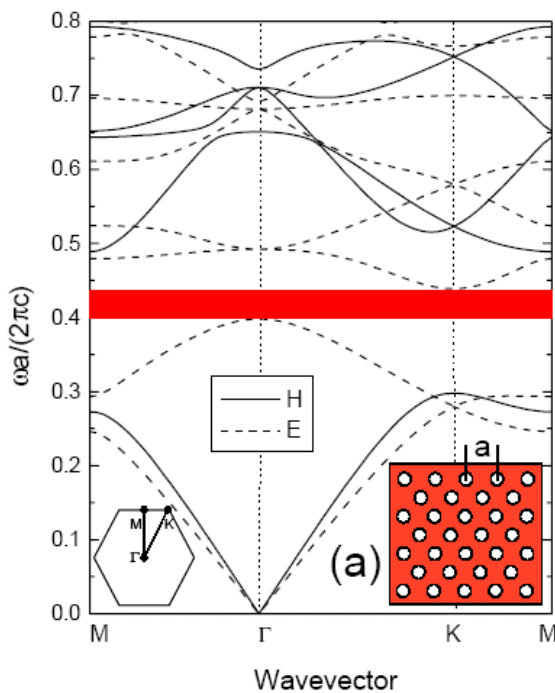


**Gap for H (TE) modes favoured by connected dielectric lattice (veins)**

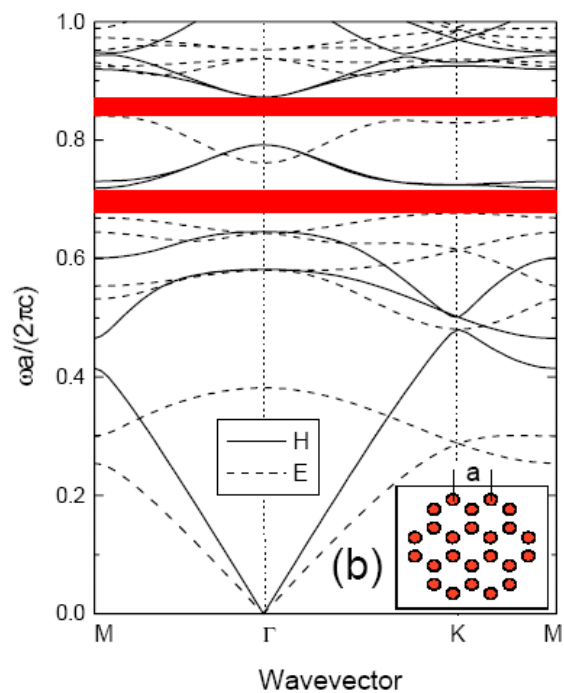
**Gap for E (TM) modes favoured by dielectric columns (pillars)**

# Complete photonic gap in 2D

Triangular lattice of holes,  $r/a=0.45$



Graphite lattice of pillars,  $r/a=0.18$



## Gap maps of triangular and graphite lattices

triangular (holes)

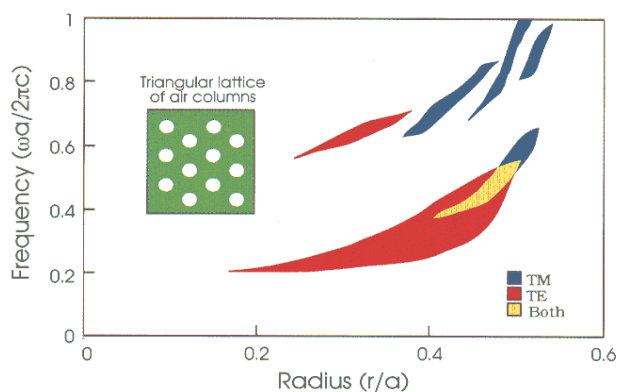


**Figure 4** Gap map for a triangular lattice of air columns drilled in a dielectric medium,  $\epsilon = 11.4$ .

graphite (pillars)

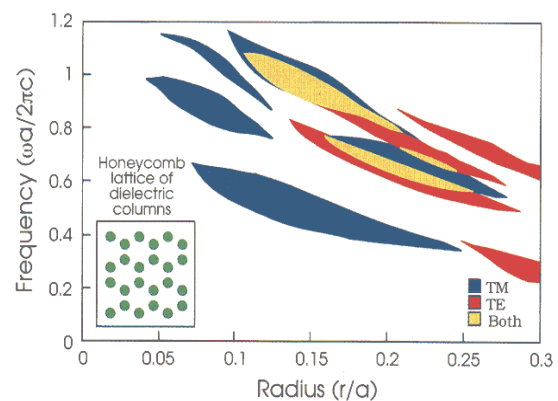


**Figure 5** Gap map for a honeycomb lattice of dielectric columns,  $\epsilon = 11.4$ .

**Gap for H (TE) modes favoured by connected dielectric lattice (holes)**

**Gap for E (TM) modes favoured by dielectric columns**

## 1. Required notions

- Basic properties of photonic band structure
- Plane-wave expansion
- Dielectric slab waveguide
- Waveguide-embedded photonic crystals

## 2. Guided-mode expansion method

- Photonic mode dispersion
- Intrinsic diffraction losses
- Convergence tests, comparison with other methods
- Examples of applications

# Books

Yariv A., *Quantum Electronics* (Wiley, New York, 1989).

Yariv A. and Yeh P., *Optical Waves in Crystals* (Wiley, New York, 1984).

Marcuse D., *Light Transmission Optics* (Van Nostrand Reinhold, New York, 1982)

Marcuse D., *Theory of Dielectric Optical Waveguides*, 2<sup>nd</sup> ed. (Academic Press, New York, 1991)

# Dielectric slab waveguide

All field components satisfy

$$\left( \nabla_{xy}^2 + \frac{\partial^2}{\partial z^2} - \varepsilon(z) \frac{\partial^2}{\partial t^2} \right) \psi = 0$$

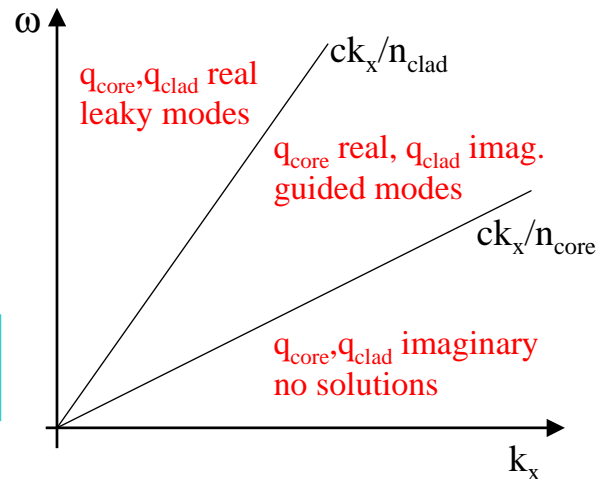
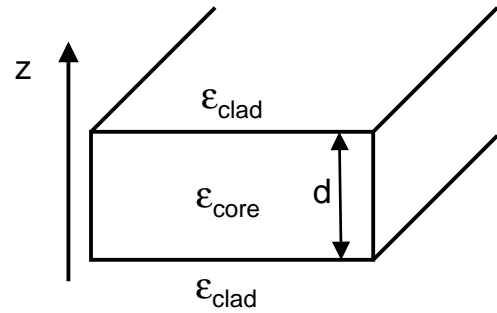
Assuming  $\psi(\mathbf{r}, t) = e^{i(k_x x - \omega t)} \psi(z)$ , we get

$$\left( \frac{\partial^2}{\partial z^2} + q^2 \right) \psi = 0, \quad q = \left( \varepsilon(z) \frac{\omega^2}{c^2} - k_x^2 \right)^{1/2}$$

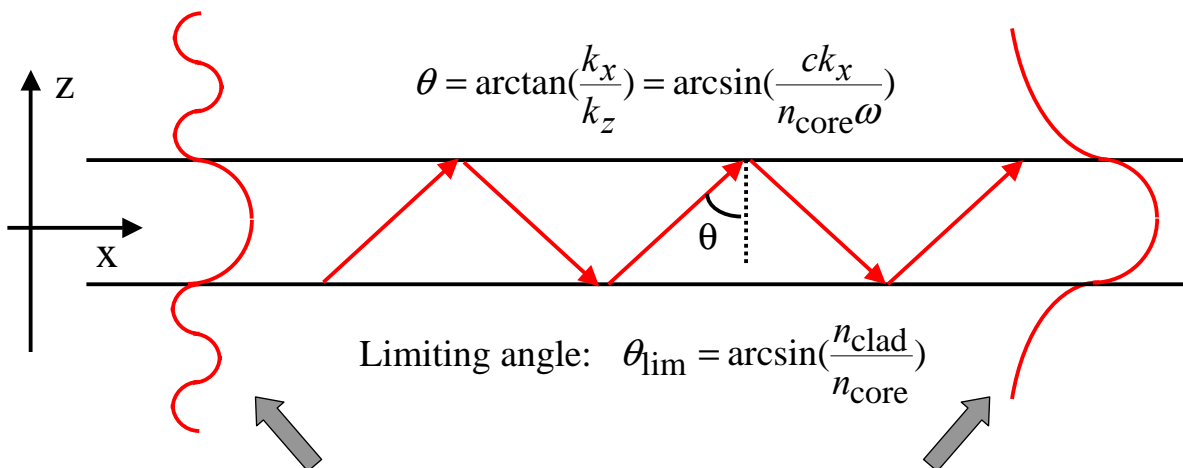
$\omega > ck_x/n \Rightarrow q^2 > 0$ , propagating field

$\omega < ck_x/n \Rightarrow q^2 < 0$ , exponentially damped

**Guided modes exist when  $\varepsilon_{\text{core}} > \varepsilon_{\text{clad}}$   
(confinement by total internal reflection)**



## Leaky vs. guided modes



$$\theta < \theta_{\text{lim}} \Leftrightarrow k_x < n_{\text{clad}} \frac{\omega}{c}$$

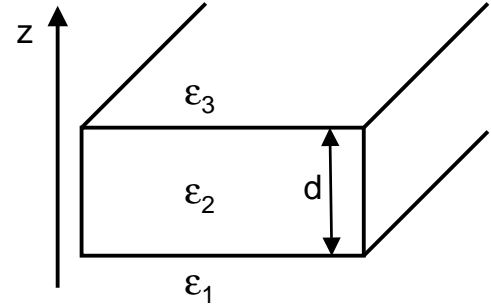
No total internal reflection, leaky mode.  
e.m. energy flux at  $z = \pm\infty$

$$\theta > \theta_{\text{lim}} \Leftrightarrow k_x > n_{\text{clad}} \frac{\omega}{c}$$

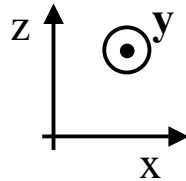
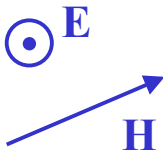
Total internal reflection, guided mode. e.m. energy flux only in xy plane

# Dielectric slab waveguide: polarizations

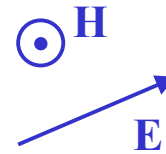
Taking the in-plane wavevector  $\mathbf{k} = k_x \hat{x}$ , the  $xz$  plane is a mirror plane and specular reflection  $\hat{\sigma}_{xz}$  is a symmetry operation (even if the slab is asymmetric in the vertical direction). Thus all modes (leaky and guided) separate into



TE modes:  $E_y, H_x, H_z$   
(odd under  $\hat{\sigma}_{xz}$ )

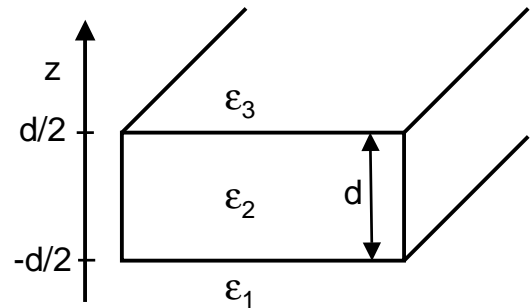


TM modes:  $H_y, E_x, E_z$   
(even under  $\hat{\sigma}_{xz}$ )



## TE guided modes

The transverse field component  $E_y$ , assuming  $E_y(\mathbf{r}, t) = e^{i(k_x x - \omega t)} E_y(z)$ , is found as



$$E_y(z) = \begin{cases} A_3 e^{-\chi_3(z-d/2)}, & \chi_3 = (k_x^2 - \epsilon_3 \frac{\omega^2}{c^2})^{1/2} & z > \frac{d}{2} \\ A_2 e^{iqz} + B_2 e^{-iqz}, & q = (\epsilon_2 \frac{\omega^2}{c^2} - k_x^2)^{1/2} & |z| < \frac{d}{2} \\ B_1 e^{\chi_1(z+d/2)}, & \chi_1 = (k_x^2 - \epsilon_1 \frac{\omega^2}{c^2})^{1/2} & z < -\frac{d}{2} \end{cases}$$

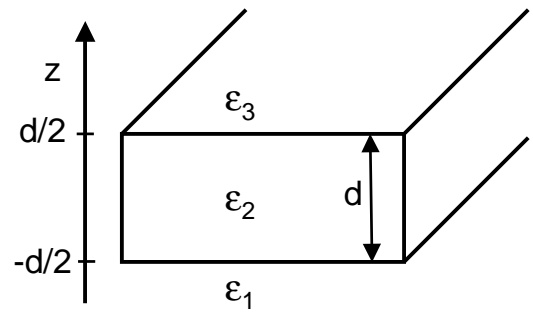
Continuity of  $E_y, H_x, H_z$  leads to the implicit equation

$$q(\chi_1 + \chi_3) \cos(qd) + (\chi_1 \chi_3 - q^2) \sin(qd) = 0$$

Relation between coefficients: *transfer-matrix method*

# TM guided modes

The transverse field component  $H_y$ , assuming  $H_y(\mathbf{r}, t) = e^{i(k_x x - \omega t)} H_y(z)$ , is found as

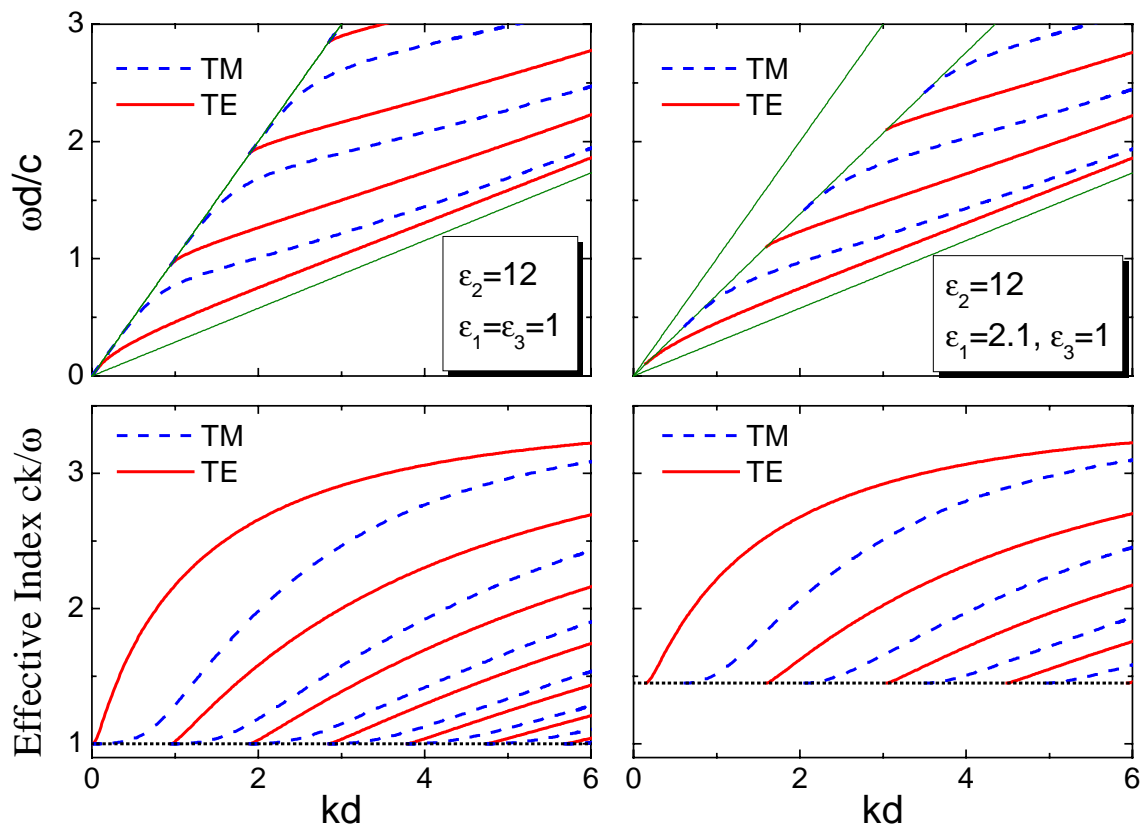


$$H_y(z) = \begin{cases} C_3 e^{-\chi_3(z-d/2)}, & \chi_3 = (k_x^2 - \epsilon_3 \frac{\omega^2}{c^2})^{1/2} & z > \frac{d}{2} \\ C_2 e^{iqz} + D_2 e^{-iqz}, & q = (\epsilon_2 \frac{\omega^2}{c^2} - k_x^2)^{1/2} & |z| < \frac{d}{2} \\ D_1 e^{\chi_1(z+d/2)}, & \chi_1 = (k_x^2 - \epsilon_1 \frac{\omega^2}{c^2})^{1/2} & z < -\frac{d}{2} \end{cases}$$

Continuity of  $H_y$ ,  $E_x$ ,  $D_z = \epsilon E_z$  leads to the implicit equation

$$\frac{q}{\epsilon_2} \left( \frac{\chi_1}{\epsilon_1} + \frac{\chi_3}{\epsilon_3} \right) \cos(qd) + \left( \frac{\chi_1 \chi_3}{\epsilon_1 \epsilon_3} - \frac{q^2}{\epsilon_2^2} \right) \sin(qd) = 0$$

## Mode dispersion and effective index



# General features of waveguide dispersion

- TM modes have higher frequencies than TE modes of the same order
- Symmetric waveguide: no cutoff for lowest-order TE and TM modes ( $\Rightarrow$  there is at least one confined photonic state at each frequency and for each polarization)
- Asymmetric waveguide: finite cutoffs even for lowest-order TE and TM modes, all cutoffs are polarization-dependent
- Effective mode index increases smoothly from cladding refractive index (close to cutoff, guided mode extends into claddings) to core refractive index (at large wavevectors, guided mode is well confined)

## 1. Required notions

- Basic properties of photonic band structure
- Plane-wave expansion
- Dielectric slab waveguide
- Waveguide-embedded photonic crystals

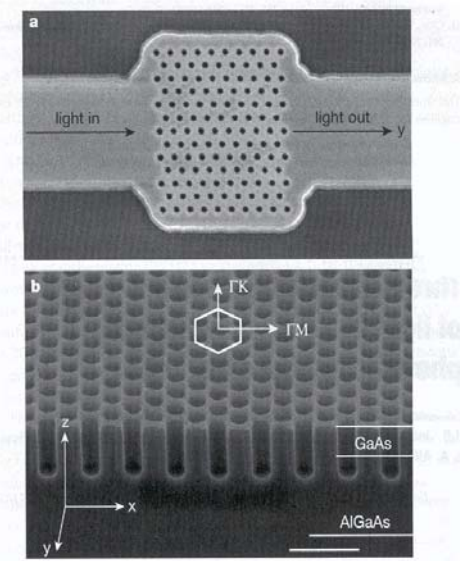
## 2. Guided-mode expansion method

- Photonic mode dispersion
- Intrinsic diffraction losses
- Convergence tests, comparison with other methods
- Examples of applications

## 2D photonic crystals embedded in planar waveguides (photonic crystal slabs)

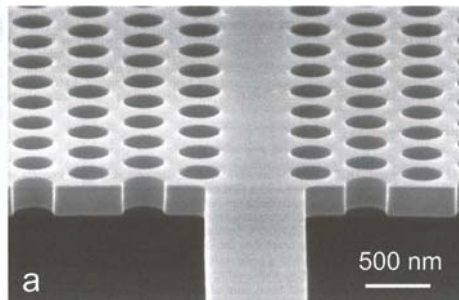
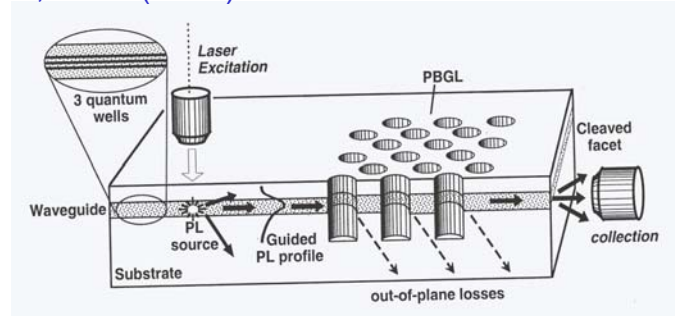
### GaAs membrane (air bridge)

Chow et al., Nature **407**, 983 (2000)



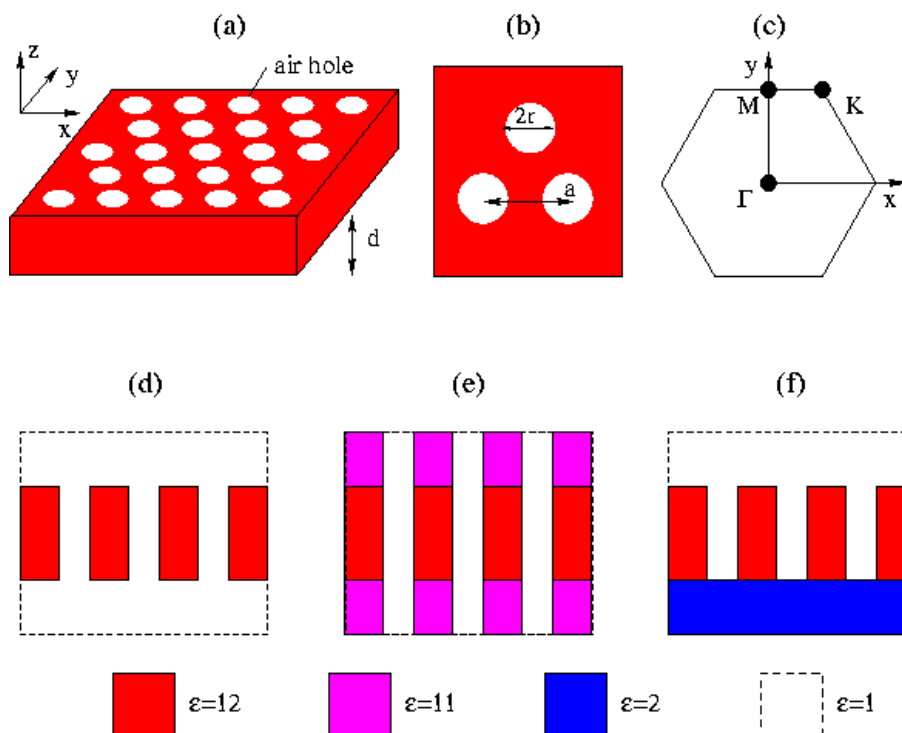
### GaAs/AlGaAs PhC slab with internal source

H. Benisty et al, IEEE J. Lightwave Technol. **17**, 2063 (1999)



**W1 waveguide  
in Si membrane**  
S.J. McNab et al,  
Opt. Expr. 11,  
2923 (2003)

## Photonic crystal slabs: structures



Air bridge

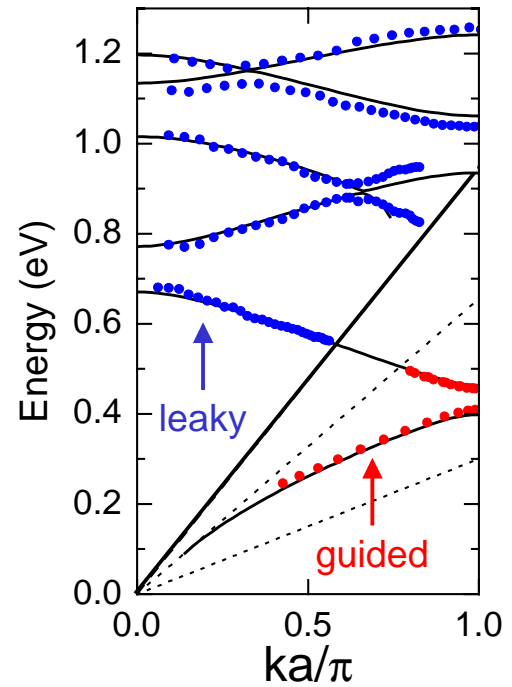
GaAs/AlGaAs

Silicon-on-Insulator (SOI)



# Photonic crystal slabs: the light-line issue

- Only modes that lie *below the light line* of the cladding material are guided with no intrinsic losses → *truly guided modes*.
- Modes that lie *above the light line* have an intrinsic loss mechanism due to out-of-plane diffraction → *quasi-guided modes*.
- The issue of *losses* (intrinsic vs. extrinsic) is a crucial one for prospective applications of PhC slabs to integrated optics.



## 1. Required notions

- Basic properties of photonic band structure
- Plane-wave expansion
- Dielectric slab waveguide
- Waveguide-embedded photonic crystals

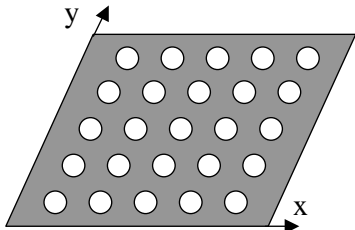
## 2. Guided-mode expansion method

- Photonic mode dispersion
- Intrinsic diffraction losses
- Convergence tests, comparison with other methods
- Examples of applications

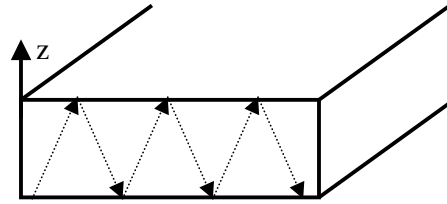
# Basic idea of guided-mode expansion

Photonic crystal slabs combine the features of

2D photonic crystals:  
control of light  
propagation in the xy  
plane by Bragg  
diffraction



Slab waveguides: control  
of light propagation in the  
vertical (z) direction by  
total internal reflection



⇒ represent the electromagnetic field as a combination of 2D plane waves in xy and guided modes along z

## General eigenvalue problem

- Equation for the magnetic field: 
$$\nabla \times \left( \frac{1}{\epsilon(\mathbf{r})} \nabla \times \mathbf{H}(\mathbf{r}) \right) = \frac{\omega^2}{c^2} \mathbf{H}(\mathbf{r})$$
  
with the transversality condition  $\nabla \cdot \mathbf{H} = 0$ .
- Expand magnetic field in a set of basis states as  $\mathbf{H}(\mathbf{r}) = \sum_{\mu} c_{\mu} \mathbf{H}_{\mu}(\mathbf{r})$ ,  
orthonormal according to  $\int \mathbf{H}_{\mu}^*(\mathbf{r}) \cdot \mathbf{H}_{\nu}(\mathbf{r}) d\mathbf{r} = \delta_{\mu\nu}$ .
- We obtain a linear eigenvalue problem with a “Hamiltonian” matrix,

$$\sum_{\nu} H_{\mu\nu} c_{\nu} = \frac{\omega^2}{c^2} c_{\mu}$$

$$H_{\mu\nu} = \int \epsilon^{-1}(\mathbf{r}) (\nabla \times \mathbf{H}_{\mu}^*(\mathbf{r})) \cdot (\nabla \times \mathbf{H}_{\nu}(\mathbf{r})) d\mathbf{r}$$

whose eigenvalues and eigenvectors give the photonic band dispersion and magnetic field, respectively.

# Electric field and normalization

Once the magnetic field is obtained, the electric field is calculated as

$$\mathbf{E}(\mathbf{r}) = i \frac{c}{\omega \epsilon(\mathbf{r})} \nabla \times \mathbf{H}(\mathbf{r}).$$

The eigenmodes  $\mathbf{E}_n(\mathbf{r})$ ,  $\mathbf{H}_n(\mathbf{r})$  of the electromagnetic field are orthonormal according to

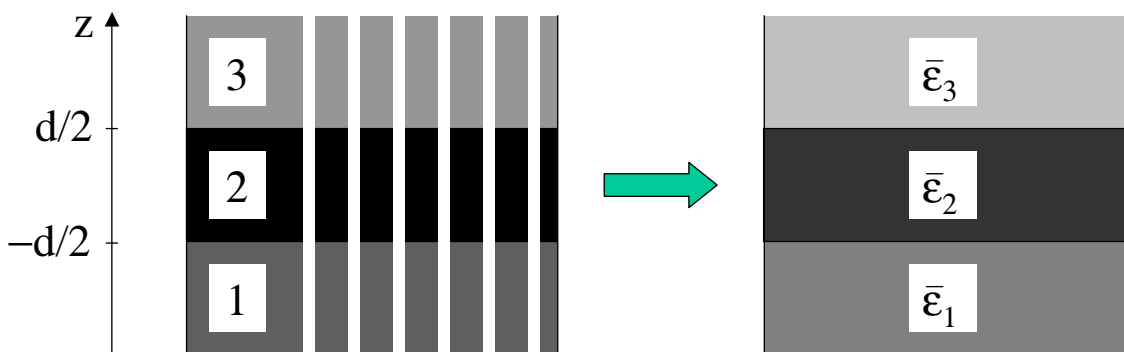
$$\begin{aligned} \int \mathbf{H}_n^*(\mathbf{r}) \cdot \mathbf{H}_m(\mathbf{r}) d\mathbf{r} &= \delta_{nm}, \\ \int \mathbf{E}_n^*(\mathbf{r}) \cdot \mathbf{E}_m(\mathbf{r}) \epsilon(\mathbf{r}) d\mathbf{r} &= \delta_{nm}. \end{aligned}$$

Physical meaning: the e.m. field energy of an eigenmode is equally shared between the electric and magnetic fields.

The same relations can be used for second quantization of the fields: see C.K. Carniglia and L. Mandel, Phys. Rev. D 3, 280 (1971).

## Effective waveguide

We consider a PhC slab with semi-infinite claddings. For the basis states  $\mathbf{H}_\mu(\mathbf{r})$ , we choose the guided modes of an effective homogeneous waveguide with an average dielectric constant  $\bar{\epsilon}_j$  in each layer  $j=1,2,3$ .



We usually take  $\bar{\epsilon}_j$  to be the spatial average of  $\epsilon_j(\mathbf{r}) \equiv \epsilon_j(\boldsymbol{\rho})$  in each layer:

$$\bar{\epsilon}_j = \frac{1}{A} \int_{\text{cell}} \epsilon_j(\boldsymbol{\rho}) d\boldsymbol{\rho}, \quad A = \text{unit cell area}$$

The average dielectric constants must fulfill  $\bar{\epsilon}_2 > \bar{\epsilon}_1, \bar{\epsilon}_3$ .

# Expansion in the basis of guided modes

$$\mathbf{H}_{\mathbf{k}}(\mathbf{r}) = \sum_{\mathbf{G}, \alpha} c(\mathbf{k} + \mathbf{G}, \alpha) \mathbf{H}_{\mathbf{k}+\mathbf{G}, \alpha}^{\text{guided}}(\mathbf{r})$$

$\mathbf{k}$  = Bloch vector, chosen to be in the first Brillouin zone

$\mathbf{G}$  = reciprocal lattice vectors of the 2D Bravais lattice

$\alpha$  = index of guided mode

$\mathbf{H}_{\mathbf{k}+\mathbf{G}, \alpha}^{\text{guided}}(\mathbf{r})$  = guided modes of effective waveguide at  $\mathbf{k}+\mathbf{G}$

Dimension of linear eigenvalue problem is  $(N_{\text{PW}} N_{\alpha}) \times (N_{\text{PW}} N_{\alpha})$ .

Since the guided modes are simple trigonometric functions, the matrix elements can be calculated analytically.

Both TE and TM guided modes appear in the expansion of a PhC slab mode. The index  $\alpha$  includes mode order and polarization.

## Matrix elements: the dielectric tensor

The matrix elements between guided modes depend on the inverse dielectric matrices in the three layers,

$$\eta_j(\mathbf{G}, \mathbf{G}') = \frac{1}{A} \int \varepsilon_j^{-1}(\boldsymbol{\rho}) e^{i(\mathbf{G}' - \mathbf{G}) \cdot \boldsymbol{\rho}} d\boldsymbol{\rho}$$

Like in 2D plane-wave expansion, they are evaluated from numerical inversion of the direct dielectric matrices:

$$\eta_j(\mathbf{G}, \mathbf{G}') = [\varepsilon_j(\mathbf{G}, \mathbf{G}')]^{-1}$$

$$\varepsilon_j(\mathbf{G}, \mathbf{G}') = \frac{1}{A} \int \varepsilon_j(\boldsymbol{\rho}) e^{i(\mathbf{G}' - \mathbf{G}) \cdot \boldsymbol{\rho}} d\boldsymbol{\rho}$$

Convergence properties, possible optimization beyond the Ho-Chan-Soukoulis procedure are similar to 2D plane-wave expansion.

The off-diagonal components of  $\eta_j(\mathbf{G}, \mathbf{G}')$  are responsible for the folding of photonic bands in the first BZ, gap formation, splittings etc.

→ mat. el.

# Discussion of GME method (dispersion)

**Main drawback:** the basis set of guided modes of the effective waveguide is not complete, since leaky modes are not included

⇒ the GME method is an APPROXIMATE one

**Main advantage:** folded photonic modes in the first Brillouin zone may fall above the light line ⇒ guided and quasi-guided photonic modes are obtained, without the need of introducing any artificial layers (PML...) in the vertical direction.

When a few guided modes are sufficient, as it often happens, the numerical effort is comparable to that of a 2D plane-wave calculation. Very suited for parameter optimization, design...

The dispersion of photonic bands in a PhC slab can be compared with that of the ideal 2D system and with the dispersion of free waveguide modes. Multimode slabs are naturally treated.

## Symmetry properties, TE/TM mixing

When the PhC slab is symmetric under reflection in the xy plane: separation of even ( $\sigma_{xy}=+1$ ) and odd ( $\sigma_{xy}=-1$ ) modes

		$\mathbf{k} = k\hat{x}$	$E_x$	$E_y$	$E_z$	$H_x$	$H_y$	$H_z$
$q \sin \frac{qd}{2} - \chi_1 \cos \frac{qd}{2} = 0$	TE, $\sigma_{xy} = +1$	TE, $\sigma_{xy} = +1$	*	+	*	-	*	+
$q \cos \frac{qd}{2} + \chi_1 \sin \frac{qd}{2} = 0$	TE, $\sigma_{xy} = -1$	TE, $\sigma_{xy} = -1$	*	-	*	+	*	-
$\frac{q}{\bar{\epsilon}_2} \cos \frac{qd}{2} + \frac{\chi_1}{\bar{\epsilon}_1} \sin \frac{qd}{2} = 0$	TM, $\sigma_{xy} = +1$	TM, $\sigma_{xy} = +1$	+	*	-	*	-	*
$\frac{q}{\bar{\epsilon}_2} \sin \frac{qd}{2} - \frac{\chi_1}{\bar{\epsilon}_1} \cos \frac{qd}{2} = 0$	TM, $\sigma_{xy} = -1$	TM, $\sigma_{xy} = -1$	-	*	+	*	+	*

Low-lying photonic modes are dominated by lowest-order modes of the effective waveguide:

$\sigma_{xy}=+1$  modes are dominated by TE waveguide modes → quasi-TE

$\sigma_{xy}=-1$  modes are dominated by TM waveguide modes → quasi-TM

However, in general, any PhC mode contains both TE and TM waveguide modes → only the symmetry labels  $\sigma_{xy}=\pm 1$  have a rigorous meaning.

## 1. Required notions

- Basic properties of photonic band structure
- Plane-wave expansion
- Dielectric slab waveguide
- Waveguide-embedded photonic crystals

## 2. Guided-mode expansion method

- Photonic mode dispersion
- Intrinsic diffraction losses
- Convergence tests, comparison with other methods
- Examples of applications

# Diffraction losses: the photonic Golden Rule

Modes above the light line are coupled to radiative PhC slab modes. Time-dependent perturbation theory, like in Fermi's golden rule for quantum mechanics, yields an imaginary part of the frequency

$$-\text{Im}\left(\frac{\omega_k^2}{c^2}\right) = \pi \sum_{\mathbf{G}', \lambda, j} |H_{\mathbf{k}, \text{rad}}|^2 \rho_j\left(\mathbf{k} + \mathbf{G}'; \frac{\omega^2}{c^2}\right).$$

The matrix element between a quasi-guided and a radiative mode is

$$H_{\mathbf{k}, \text{rad}} = \int \frac{1}{\mathcal{E}(\mathbf{r})} (\nabla \times \mathbf{H}_{\mathbf{k}}^*(\mathbf{r})) \cdot (\nabla \times \mathbf{H}_{\mathbf{k}+\mathbf{G}', \lambda, j}^{\text{rad}}(\mathbf{r})) d\mathbf{r}$$

The sum is over

- $\mathbf{G}' \rightarrow$  reciprocal lattice vectors (out-of-plane diffraction channels)
- $\lambda = \text{TE, TM} \rightarrow$  polarization of radiative PhC slab modes
- $j = 1, 3 \rightarrow$  radiative modes that are outgoing in medium 1, 3

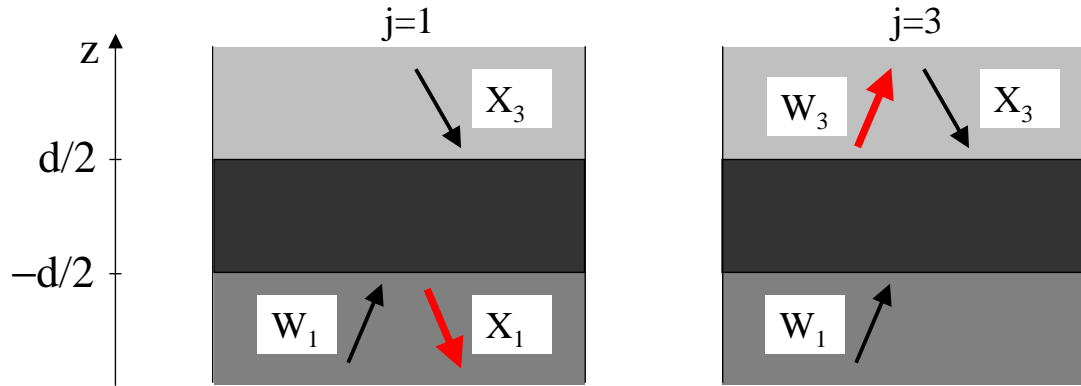
**Main approximation: radiative PhC slab modes are replaced with those of the effective waveguide.**

# Photonic DOS and scattering states

The 1D photonic density of states at fixed in-plane wavevector is

$$\rho_j\left(\mathbf{g}; \frac{\omega^2}{c^2}\right) = \int_0^\infty \frac{dk_z}{2\pi} \delta\left(\frac{\omega^2}{c^2} - \frac{g^2 + k_z^2}{\epsilon_j}\right) = \frac{(\epsilon_j)^{1/2} c}{4\pi} \frac{\theta(\omega^2 - \frac{c^2 \mathbf{g}^2}{\epsilon_j})}{(\omega^2 - \frac{c^2 \mathbf{g}^2}{\epsilon_j})^{1/2}}.$$

It depends only on the asymptotic form of the fields, for scattering states with a single **outgoing** component:



## Coupling matrix element

Using the guided-mode expansion for the magnetic field of a PhC slab mode, the matrix element with a radiative mode is

$$H_{\mathbf{k},\text{rad}} = \sum_{\mathbf{G},\alpha} c(\mathbf{k} + \mathbf{G}, \alpha)^* H_{\text{guided},\text{rad}}$$

where

$$H_{\mathbf{k},\text{rad}} = \int \frac{1}{\epsilon(\mathbf{r})} (\nabla \times \mathbf{H}_{\mathbf{k}}^*(\mathbf{r})) \cdot (\nabla \times \mathbf{H}_{\mathbf{k}+\mathbf{G}',\lambda,j}^{\text{rad}}(\mathbf{r})) d\mathbf{r}$$

are matrix elements between guided and radiation modes of the effective waveguide, which are calculated analytically.

Both guided and radiation modes are normalized according to

$$\int \mathbf{H}_{\mu}^*(\mathbf{r}) \cdot \mathbf{H}_{\nu}(\mathbf{r}) d\mathbf{r} = \delta_{\mu\nu}$$

(within a large box for radiation modes).

→ mat. el.

# Quality factor and propagation loss

The quality factor of a photonic mode is defined as

$$Q = \frac{\omega}{2\text{Im}(\omega)}.$$

Spatial attenuation is described by an imaginary part of the wavevector:

$$\text{Im}(k) = \frac{\text{Im}(\omega)}{v_g},$$

where

$$v_g = \frac{d\omega}{dk}$$

is the mode group velocity. Propagation losses in decibels are obtained as

$$\text{Loss} = 4.34 \cdot 2\text{Im}(k).$$

To treat line and point defects (linear waveguides and nanocavities):

**use a supercell**

## Discussion of GME method (losses)

**Main drawback:** radiative PhC slab modes are replaced with those of the effective homogeneous waveguide

⇒ **the calculation of losses is an APPROXIMATE one**

**Main advantage:** diffraction losses are calculated by perturbation theory → the procedure is numerically very efficient (little additional effort beyond photonic mode dispersion).

Calculated values are more accurate when diffraction losses are small → good for line defects and for high-Q nanocavities.

The method can be extended to disorder-induced losses of truly-guided modes below the light line.



## 1. Required notions

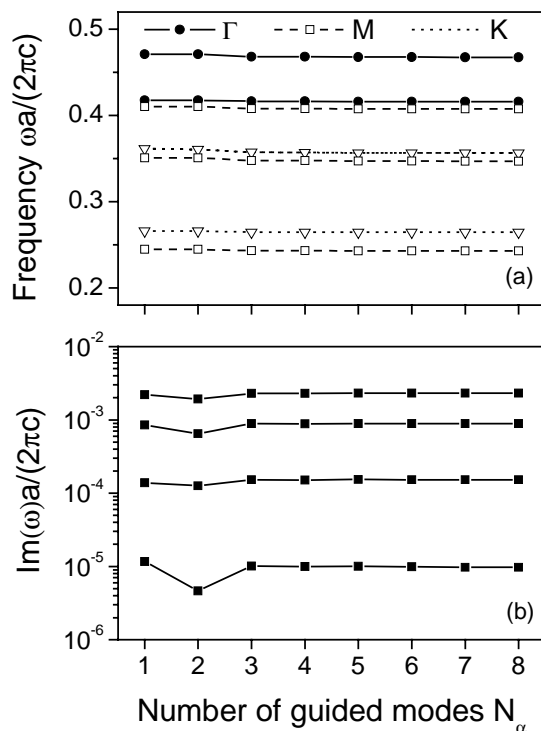
- Basic properties of photonic band structure
- Plane-wave expansion
- Dielectric slab waveguide
- Waveguide-embedded photonic crystals

## 2. Guided-mode expansion method

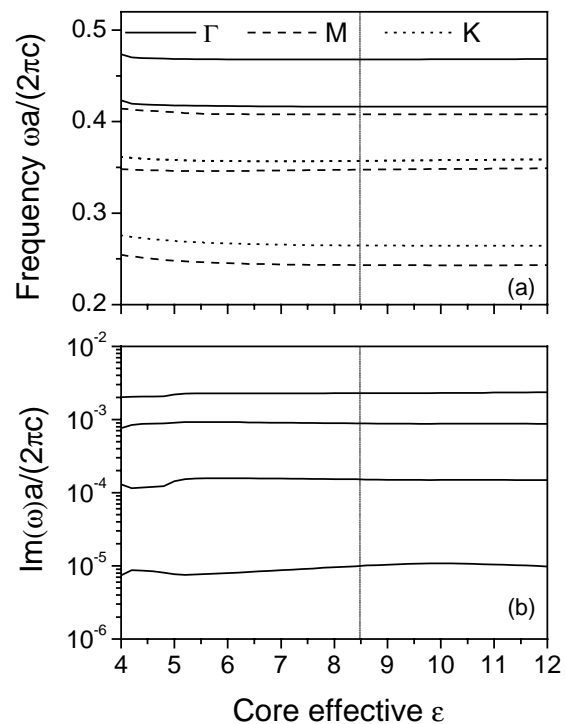
- Photonic mode dispersion
- Intrinsic diffraction losses
- Convergence tests, comparison with other methods
- Examples of applications

# Convergence tests

Triangular lattice on membrane,  $\epsilon=12.11$ ,  $d/a=0.5$ ,  $r/a=0.3$



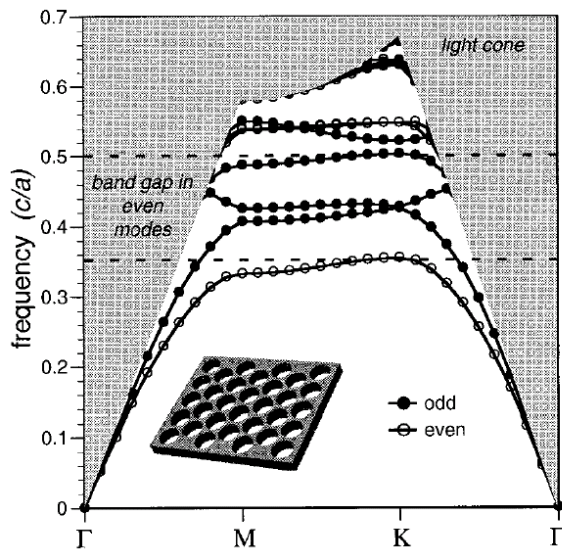
Few guided modes are sufficient for convergence



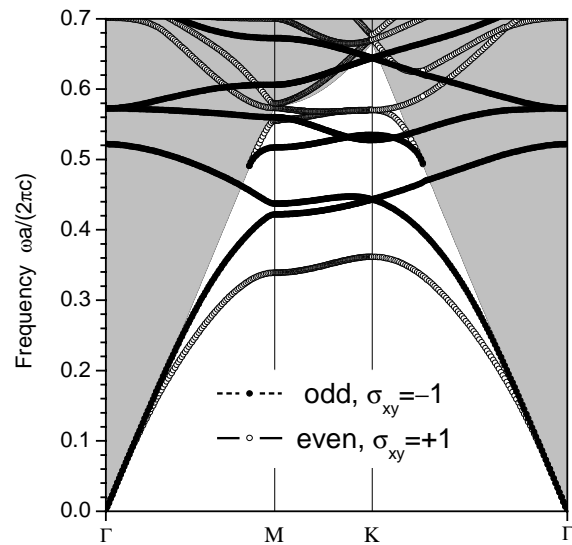
Use of average  $\epsilon$  is justified

# Comparison with MIT code

Triangular lattice on membrane,  $\epsilon=12$ ,  $d/a=0.6$ ,  $r/a=0.45$



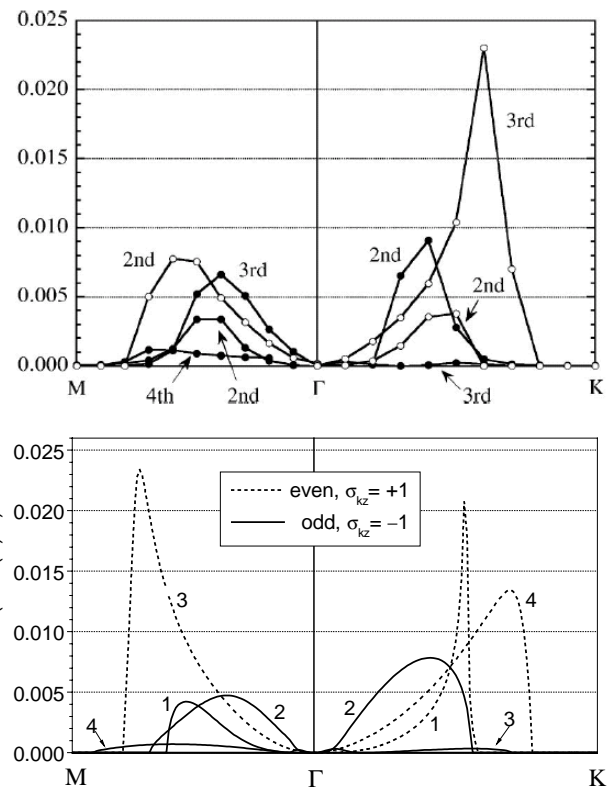
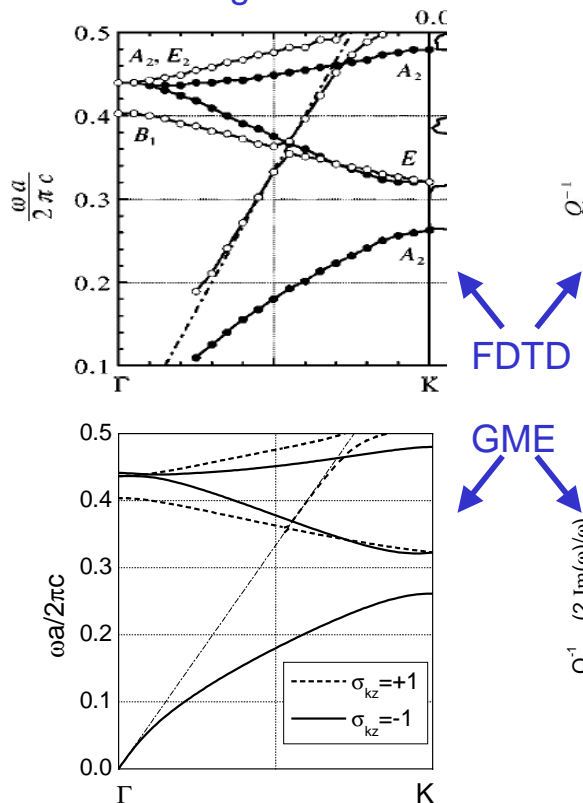
S.G. Johnson et al.,  
PRB 60, 5751 (1999)



Guided-mode expansion

# Comparison with FDTD\*

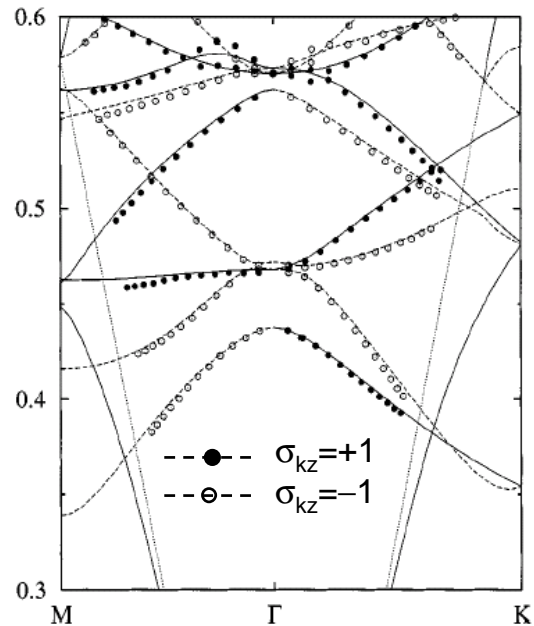
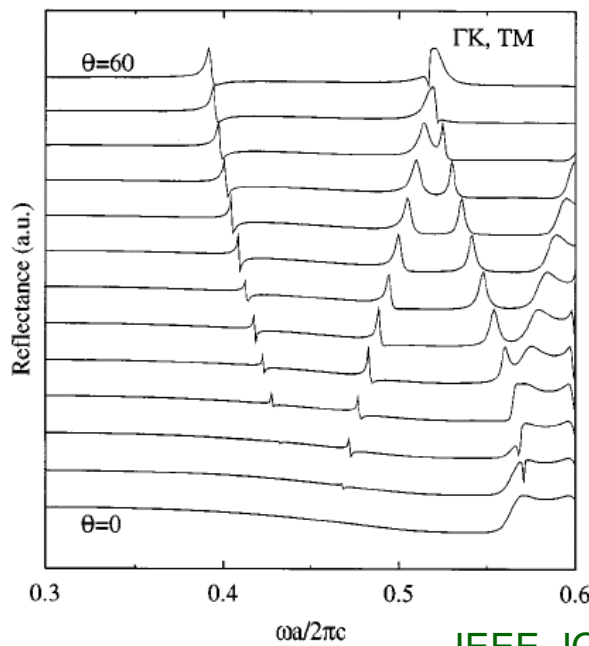
Triangular lattice on membrane,  $\epsilon=11.56$ ,  $d/a=0.65$ ,  $r/a=0.25$



\*T. Ochiai and K. Sakoda, PRB 63, 125107 (2001)

# Comparison with Fourier-modal method (scattering-matrix)

Triangular lattice on membrane,  $\epsilon=12$ ,  $d/a=0.3$ ,  $r/a=0.24$

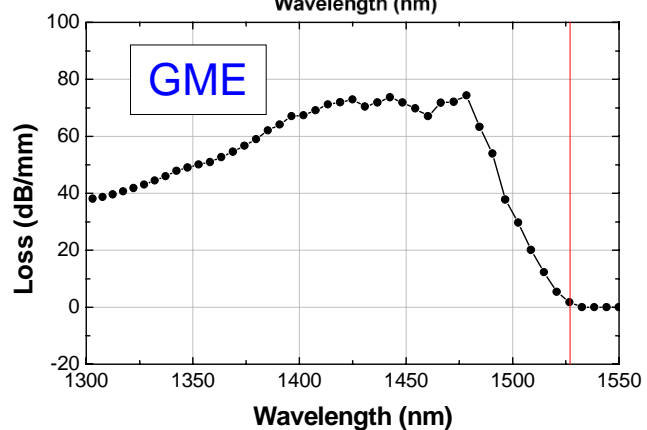
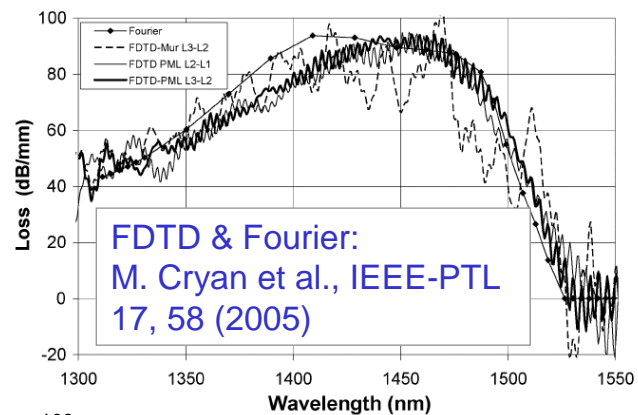
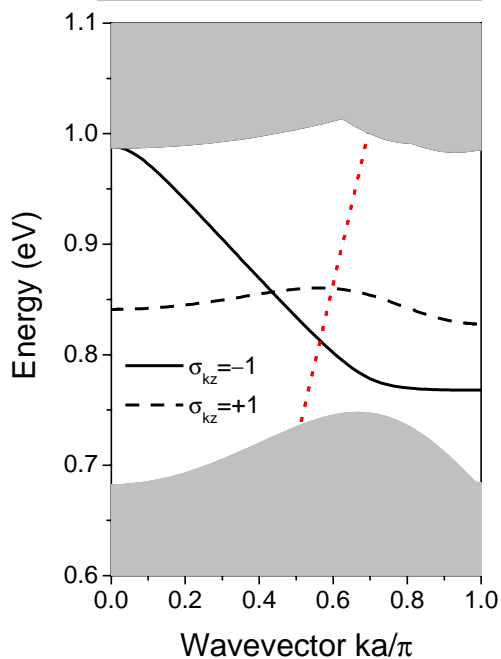


IEEE-JQE 38, 891 (2002)

N.b. Along main symmetry directions: vertical parity symmetry  $\sigma_{kz}$

## Losses in W1 waveguide: a comparison

Membrane,  $\epsilon=11.56$ ,  
 $h=0.6a$ ,  $r=0.3016a$



## 1. Required notions

- Basic properties of photonic band structure
- Plane-wave expansion
- Dielectric slab waveguide
- Waveguide-embedded photonic crystals

## 2. Guided-mode expansion method

- Photonic mode dispersion
- Intrinsic diffraction losses
- Convergence tests, comparison with other methods
- Examples of applications

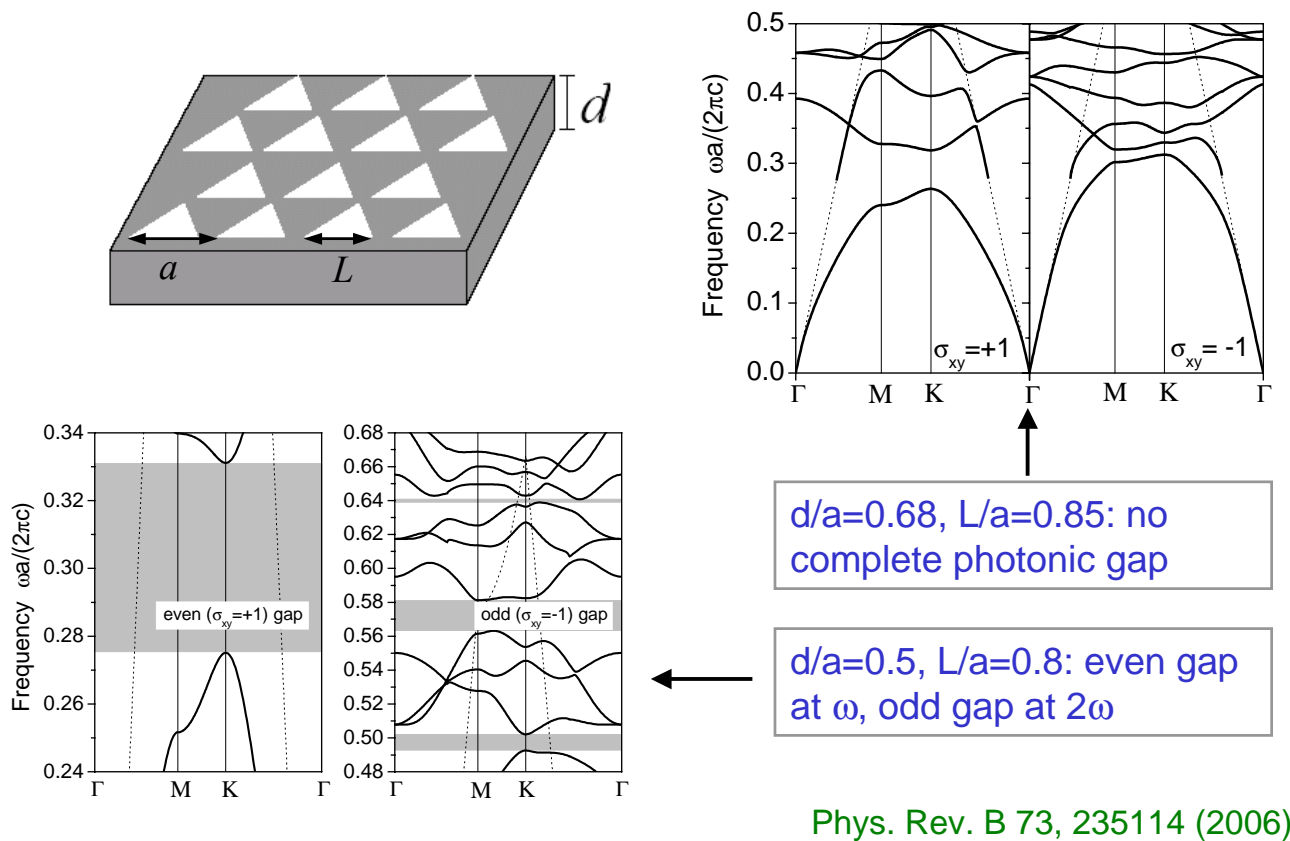
# Applications of GME method

- Photonic band dispersion and gap maps: 1D and 2D lattices
- Linear waveguides: propagation losses
- Photonic crystal nanocavities: Q-factors
- Geometry optimization, design, comparison with expts...
- Radiation-matter interaction: exciton-polaritons, strong coupling
- Extrinsic losses: effects of disorder

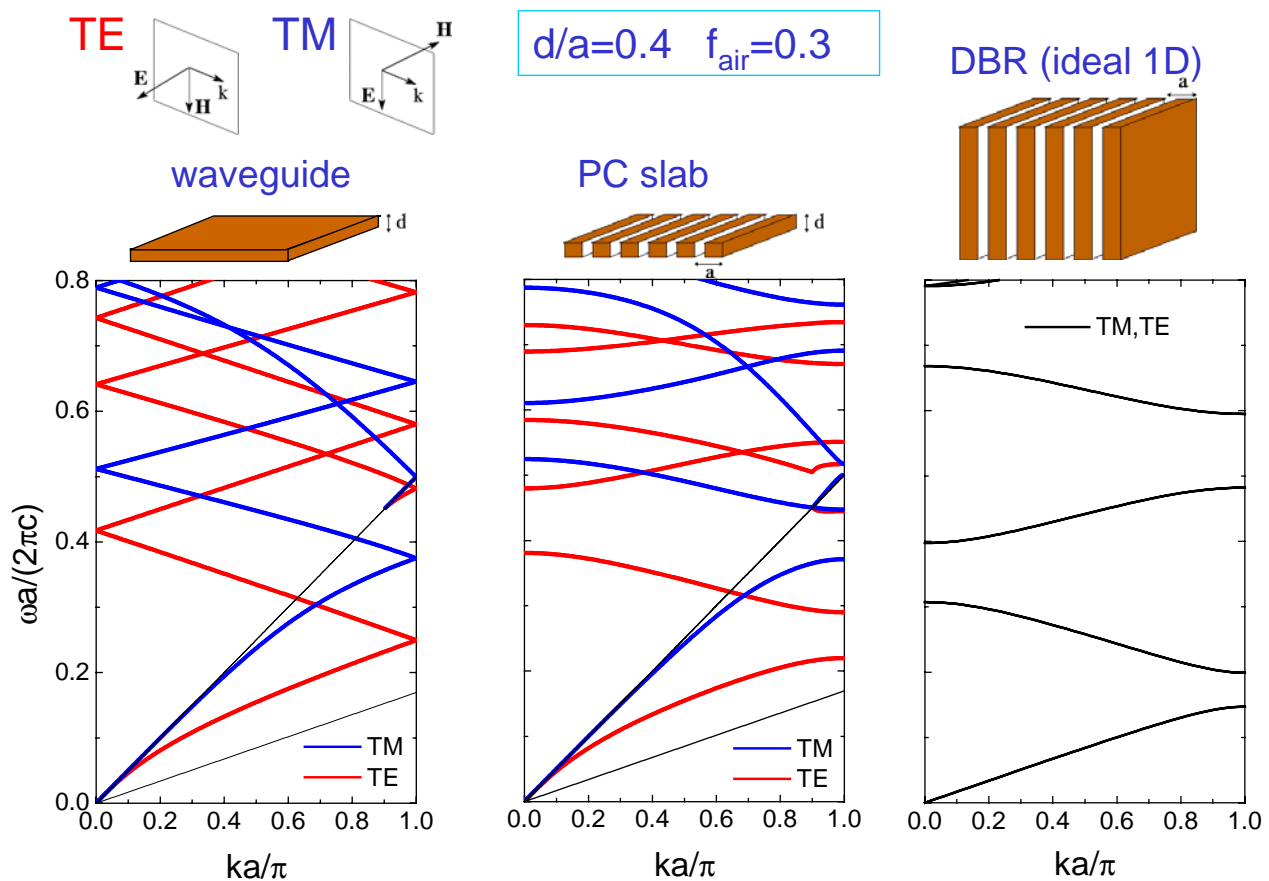
Main reference on the method:

L.C. Andreani and D. Gerace, Phys. Rev. B 73, 235114 (15 June 2006)

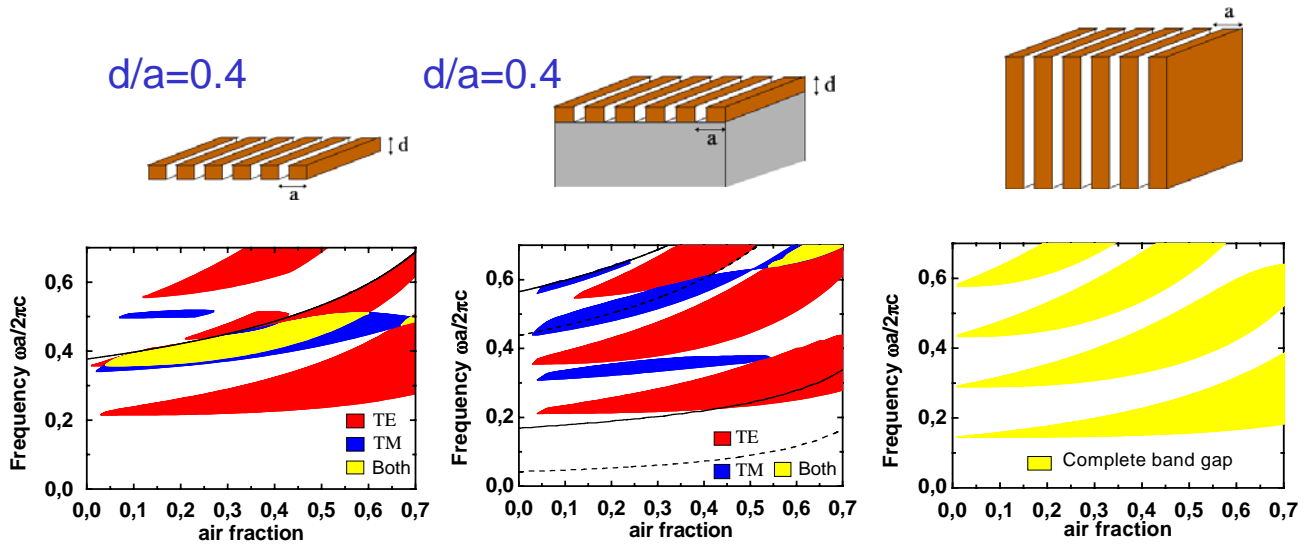
# Triangular lattice with triangular holes



# Dielectric mirror in a membrane: 1D PhC slab



# Gap maps in 1D PhC slabs

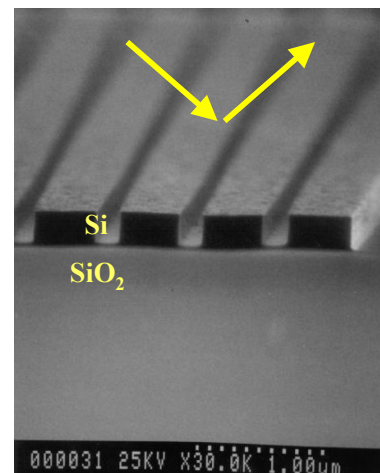
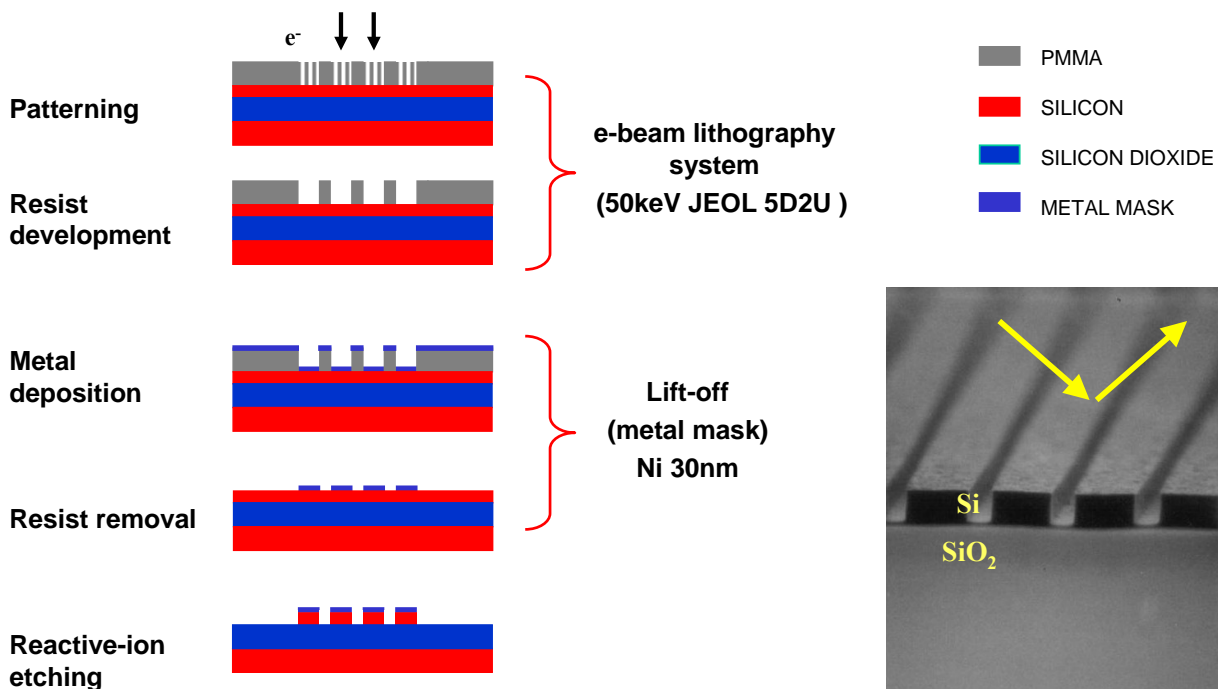


- Gap maps for PhC slabs must consider both the modes below and above the light line. Important for the design of structures with defect modes
- Very different behavior as compared to the reference ideal 1D system: no complete band gap, TE/TM splitting

D. Gerace and LCA, Phys. Rev. E 69, 056603 (2004)

## SOI photonic crystal slabs: fabrication procedure

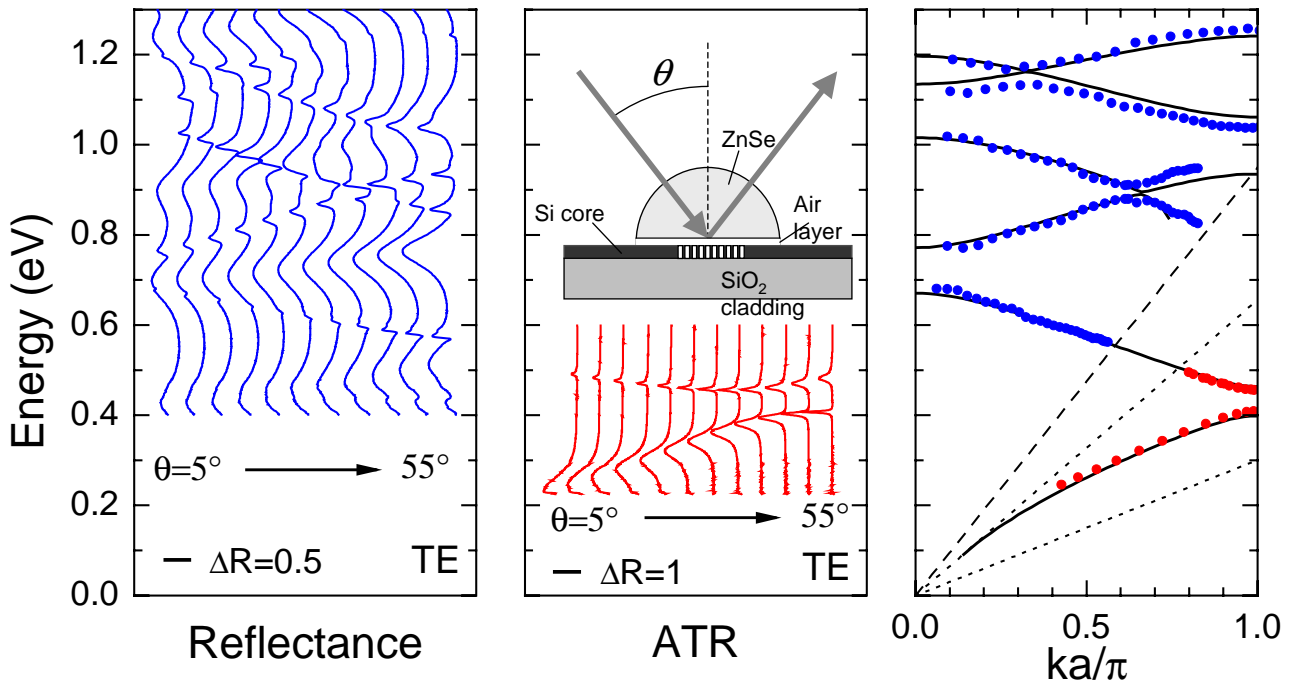
(D. Peyrade, M. Belotti and Y. Chen, LPN Marcoussis)



Sample L4

# Reflectance and ATR on 1D SOI PhC slabs

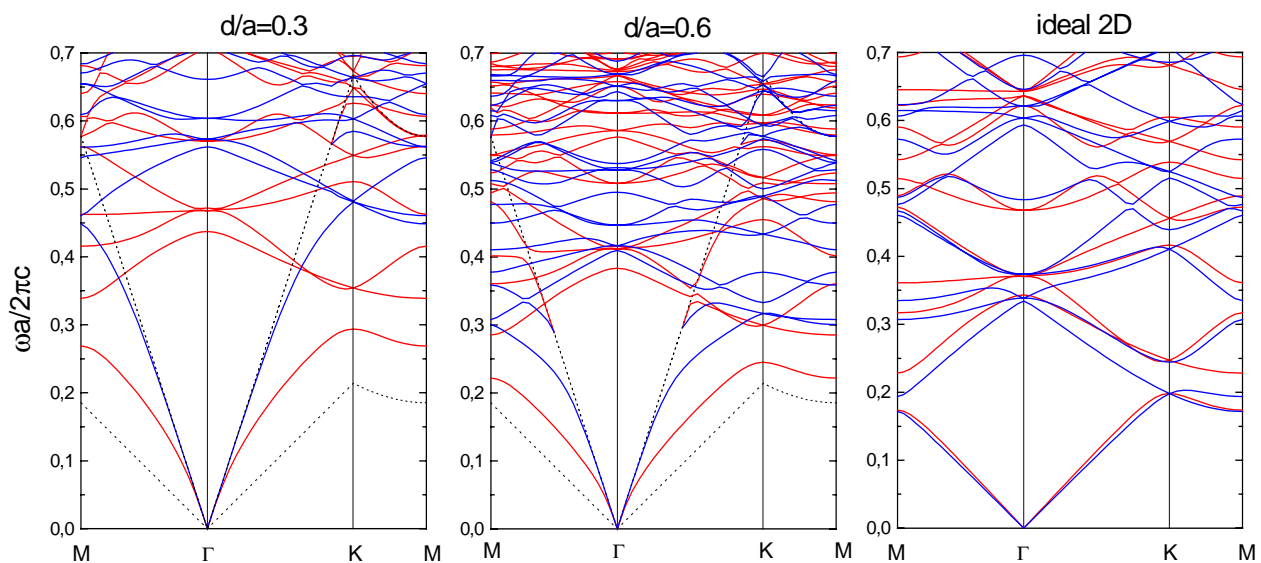
In-plane wavevector  $k_{\parallel} = n(\omega/c)\sin\theta + G \rightarrow$  photonic bands



M. Patrini et al, IEEE-JQE **38**, 885 (2002); M. Galli et al, IEEE-JSAC **23**, 1402 (2005)

## Photonic mode dispersion: air bridge

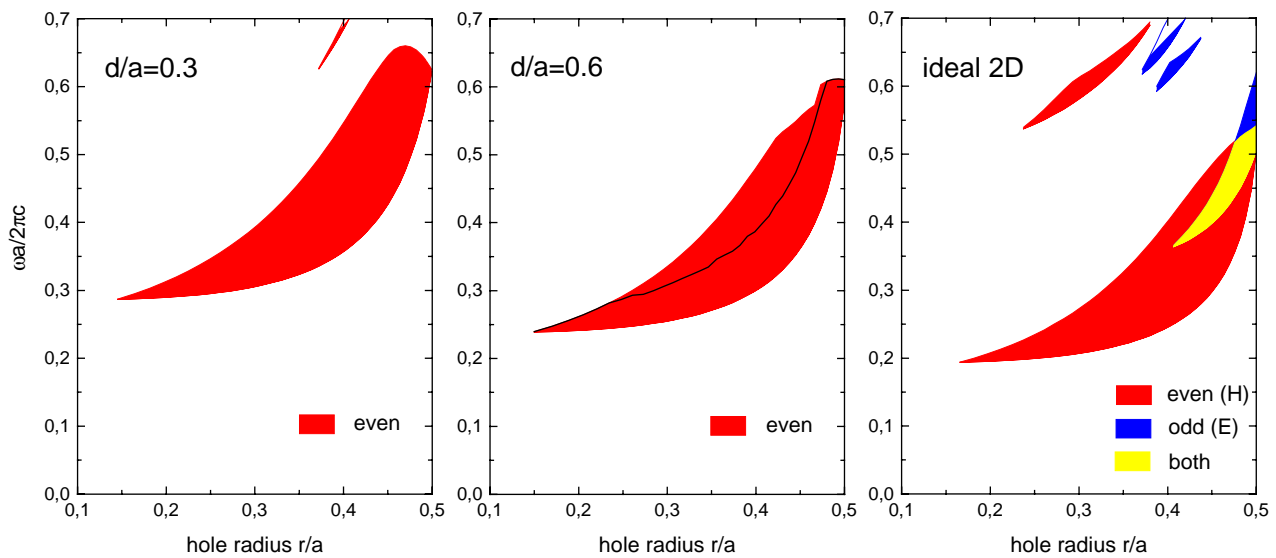
Triangular lattice, hole radius  $r=0.24a$ , different core thicknesses  $d$



Red (blue) lines  $\rightarrow$  bands that are even (odd) with respect to reflection in the  $xy$  plane.  
 Dotted lines  $\rightarrow$  dispersion of light in the effective core material and in air.  
 Notice the vertical confinement effect, which increases with decreasing core thickness.  
 Below the light line, good agreement with S.G. Johnson et al., PRB **60**, 5751 (1999).



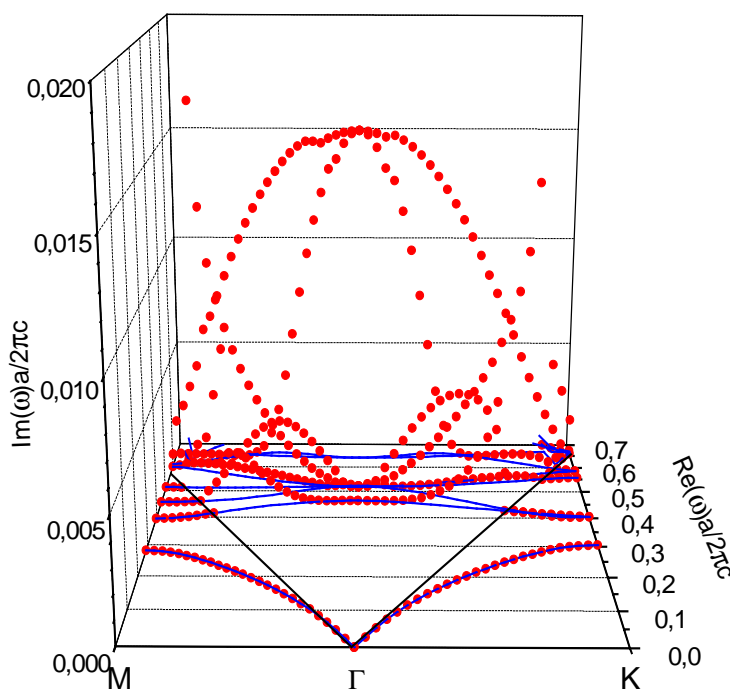
## Gap maps: triangular lattice in air bridge



Notice the confinement effect of the even gap with respect to the ideal 2D case and the absence of a full photonic band gap in a waveguide.  
For  $d/a=0.6$  the cutoff energy of a second-order mode is plotted.

L.C. Andreani and M. Agio, IEEE-JQE **38**, 891 (2002)

## 2D triangular lattice: complex energies (3D plot)



Air bridge,  $d=0.3a$ ,  $r/a=0.3$ .

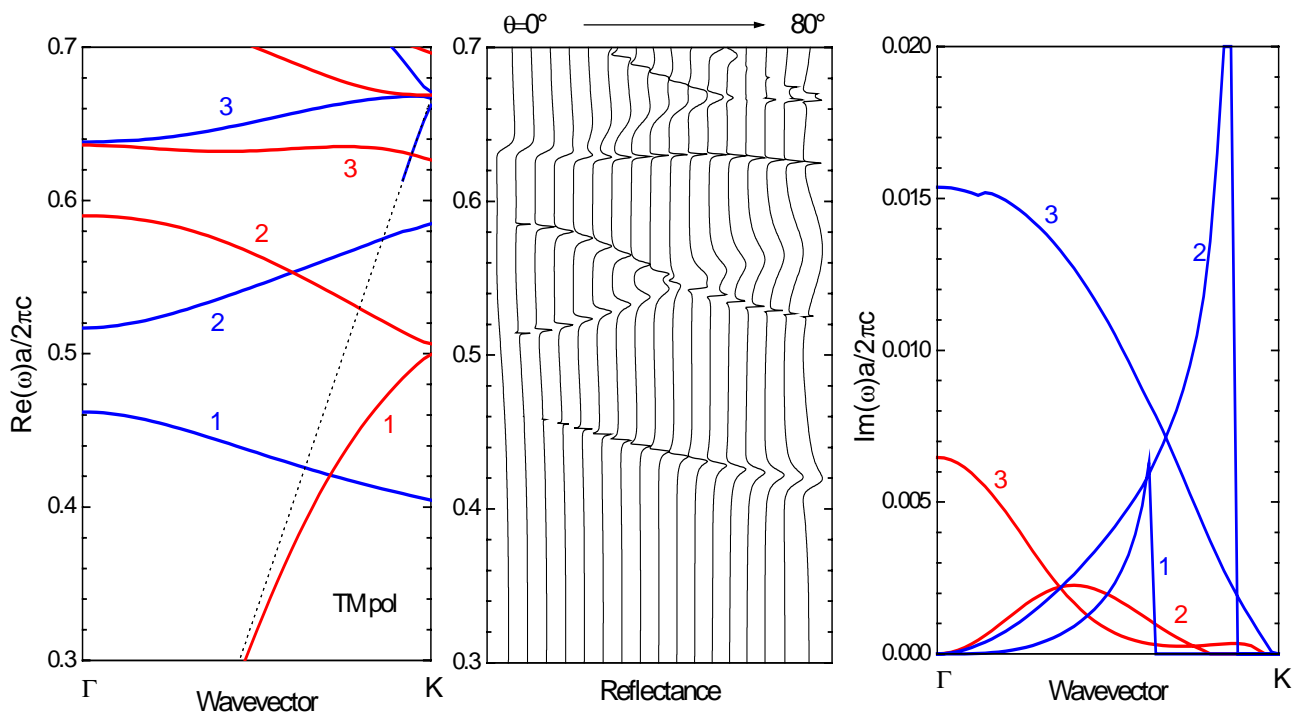
The radiative width of quasi-guided modes increases for some modes close to the light line, due to the 1D DOS.

At the  $\Gamma$  point, only the dipole-allowed mode has nonzero radiative width.

Phys. Status Solidi (b) **234**, 139 (2002)



# Complex energies vs. reflectivity



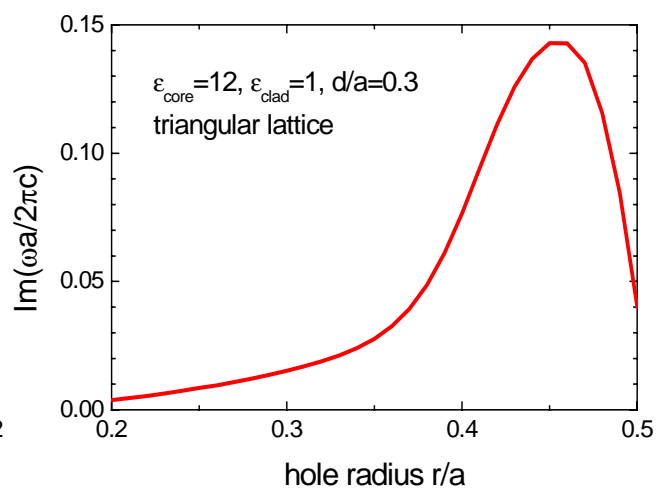
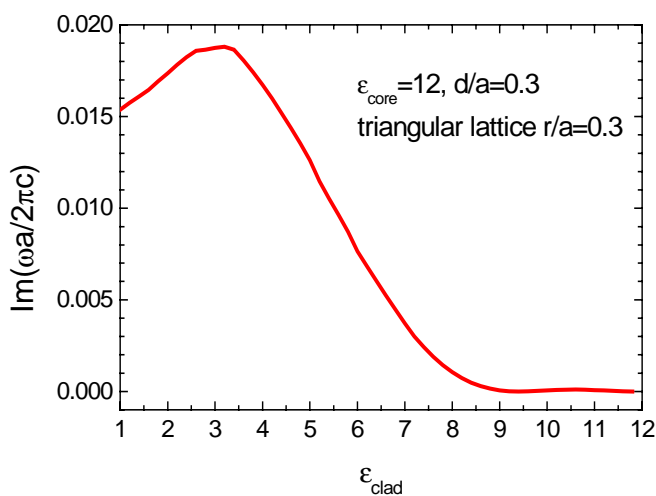
Air bridge  $d=0.3a$ , triangular lattice of holes  $r=0.3a$ ,  $\Gamma K$ , TM polarization.  
Positions and *linewidths* of spectral structures  $\rightarrow$  *real* and *imaginary* parts of energy.

Synt. Met. 139, 695 (2003)

## Trends: losses as a function of ...

... waveguide dielectric contrast

... hole radius

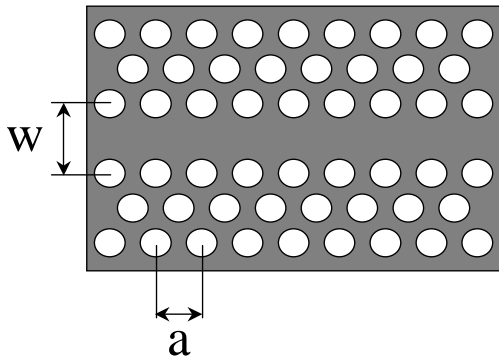


Radiative width of dipole-allowed mode at the  $\Gamma$  point.

The losses increase with the dielectric contrast between core and cladding and with the air fraction of the 2D lattice.

Agreement with the model of H. Benisty et al, APL **76**, 532 (2000).

# Linear waveguides in 2D PhC slabs



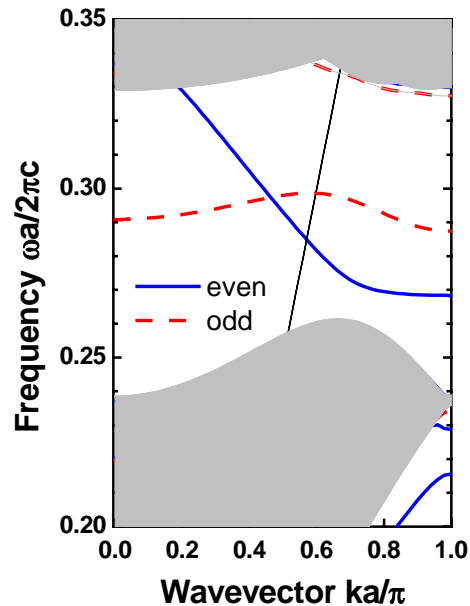
Single missing row of holes in triangular lattice, channel thickness (W1 waveguide):  $w=w_0 \equiv \sqrt{3}a$

$\epsilon=12$ ,  $d/a=0.5$ ,  $r/a=0.28$ ,  $a=400$  nm

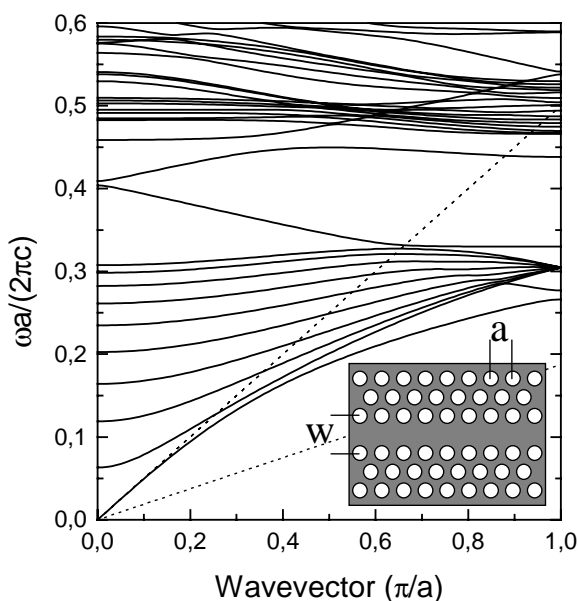
Propagation losses of truly guided modes in Si membranes (extrinsic):

$\sim 0.6$  dB/mm

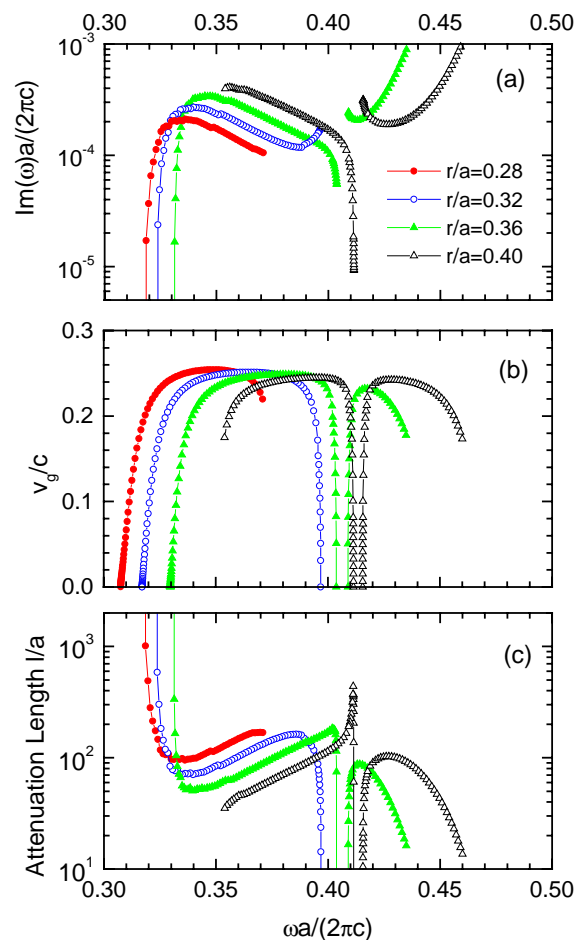
(Notomi et al., Vlasov et al.)



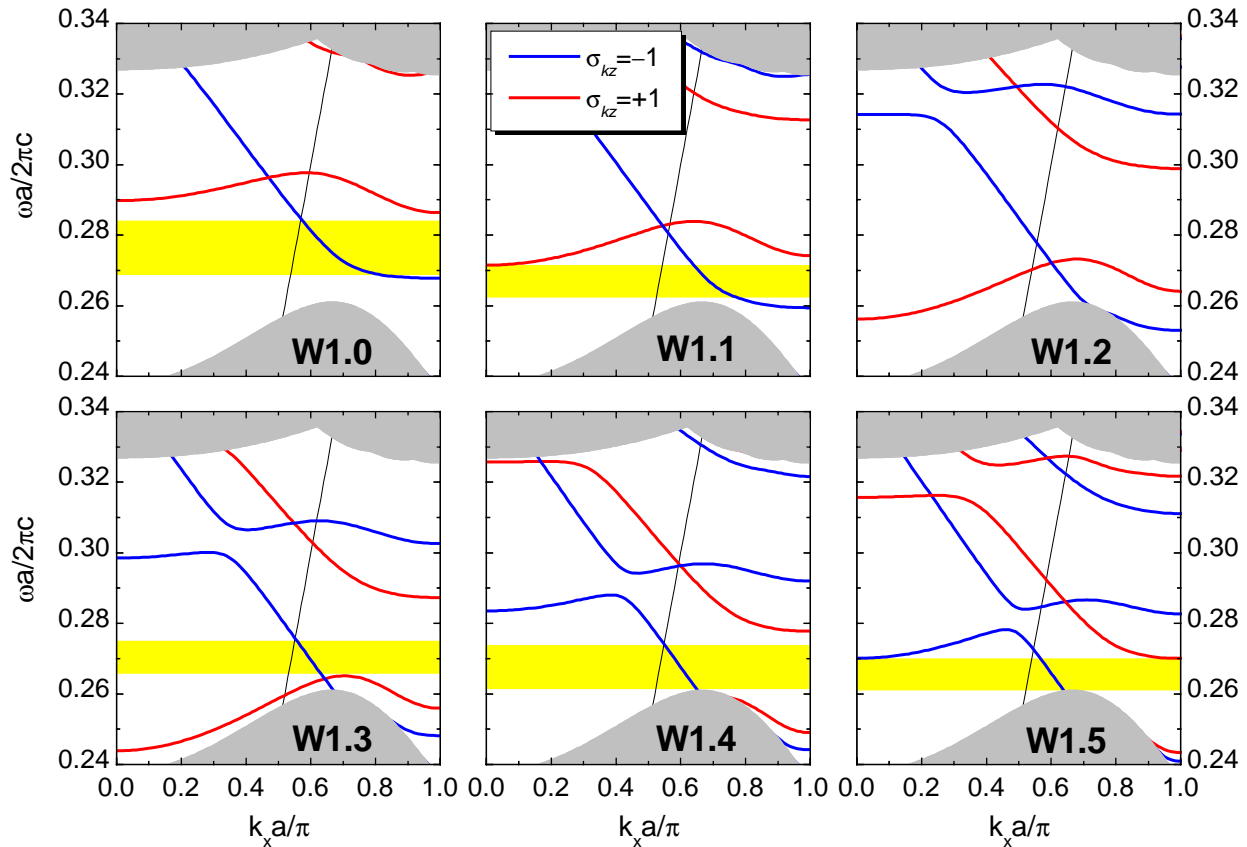
## Propagation losses in W1 waveguides



LCA and M. Agio,  
Appl. Phys. Lett. 82, 2011 (2003)

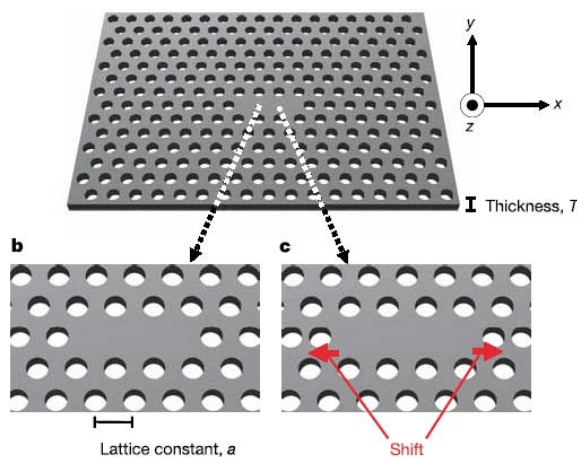


## Mode dispersion on increasing channel width

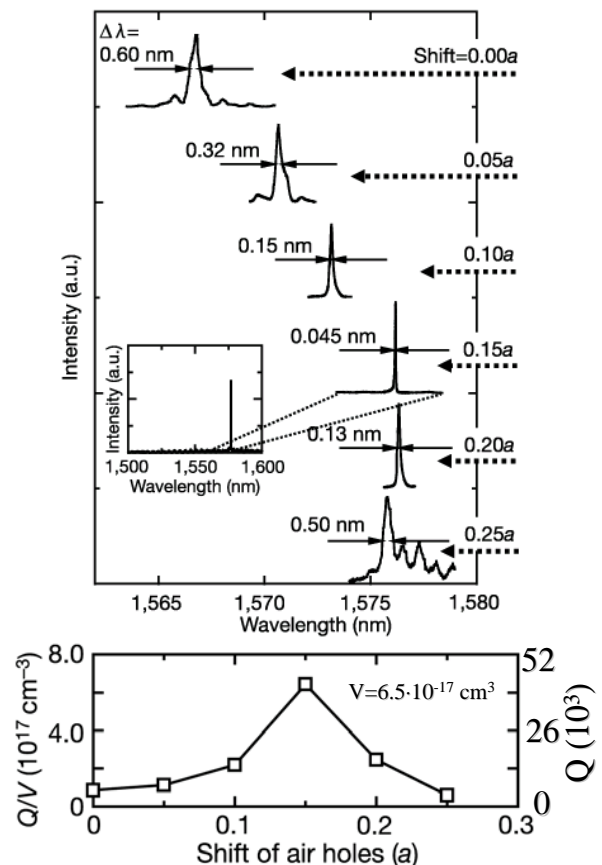


M. Galli et al., PRB 72, 125322 (2005)

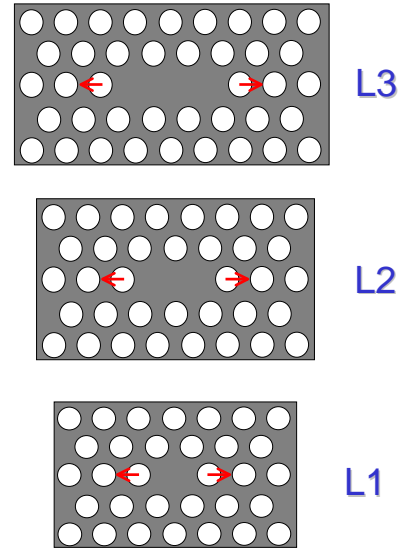
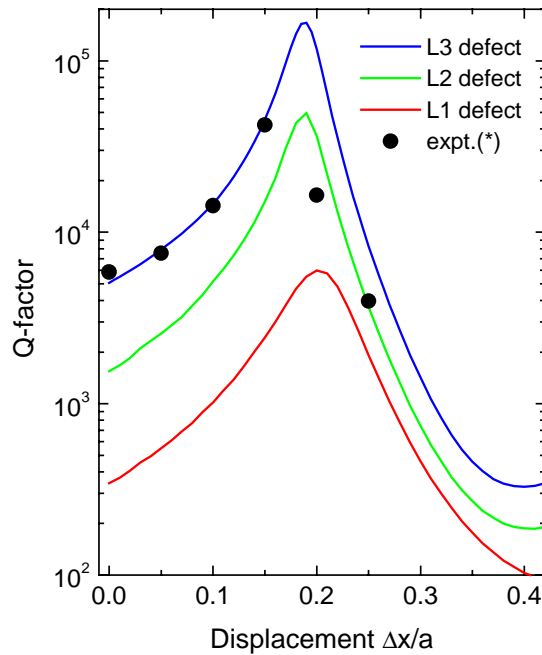
## Photonic crystal nanocavities



Point defects in PC slabs behave as 0D cavities with full photonic confinement in very small volumes. The Q-factor can be increased by shifting the positions of nearby holes.  $Q=45'000$  has been measured:  
 T. Akahane, T. Asane, B.S. Song, and S. Noda, Nature 425, 944 (2003).



# Q-factor of photonic crystal cavities



Supercell in two directions + Golden Rule  
 $\rightarrow \text{Im}(\omega)$  and  $Q = \omega / 2\text{Im}(\omega)$

\*Expt: T. Akahane et al.,  
 Nature 425, 944 (2003).

LCA, D. Gerace and M. Agio, Photonics and Nanostruc. 2, 103 (2004)

## A model of disorder: size variations

Random distribution of hole radii within a large supercell:

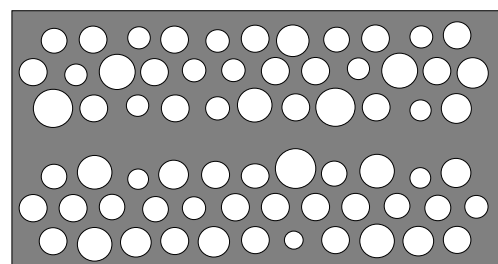
$$P(r) = \exp\left(-\frac{(r - \bar{r})^2}{2\sigma^2}\right) \quad \sigma \equiv \Delta r = \text{r.m.s. deviation}$$

Dielectric perturbation  $\Delta\epsilon(\mathbf{r}) = \epsilon_{\text{dis}}(\mathbf{r}) - \epsilon(\mathbf{r})$  couples guided modes to leaky waveguide modes  $\rightarrow$  losses by perturbation theory:

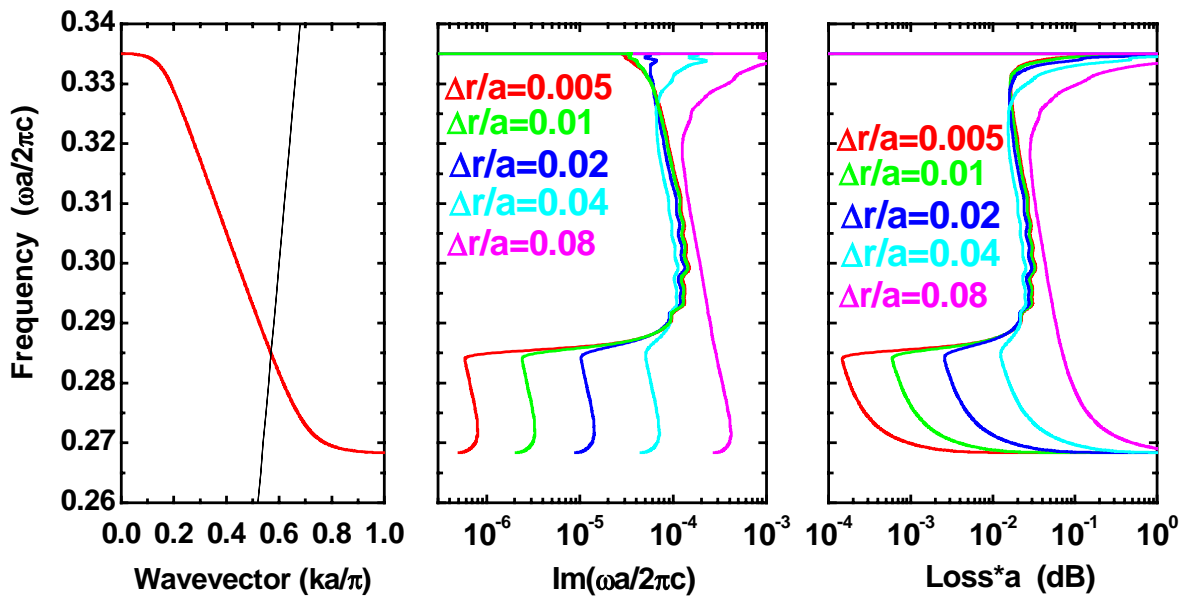
$$-\text{Im}\left(\frac{\omega_k^2}{c^2}\right) = \pi \left| \int \frac{1}{\epsilon_{\text{dis}}(\mathbf{r})} \nabla \times \mathbf{H}_{\text{leaky}}^* \cdot \nabla \times \mathbf{H}_{\text{guided}} d\mathbf{r} \right|^2 \rho\left(\mathbf{k}; \frac{\omega^2}{c^2}\right)$$

Propagation loss:

$$2\text{Im}(k) = 2 \frac{\text{Im}(\omega_k)}{v_g}, \quad v_g = \frac{d\omega_k}{dk}$$



# Dependence on disorder parameter

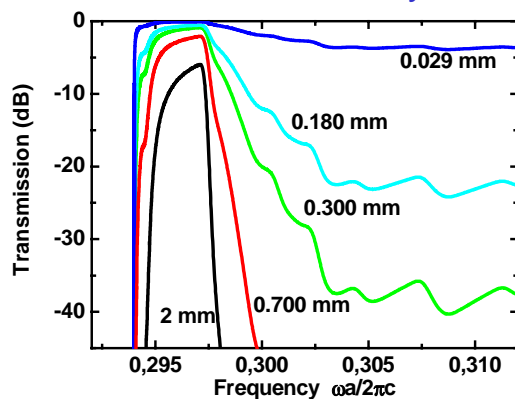


The losses show a quadratic behavior as a function of the disorder parameter...typical of Rayleigh scattering

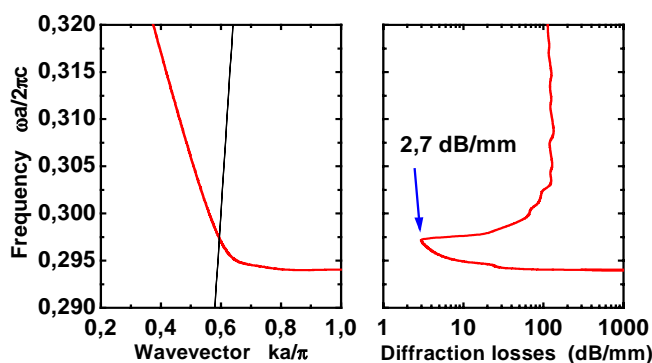
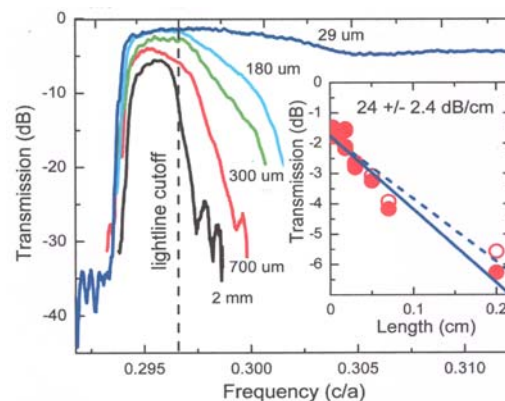
D. Gerace and L.C. Andreani, Opt. Lett. 29, 1897 (2004)

## Comparison with experimental results<sup>[1]</sup>

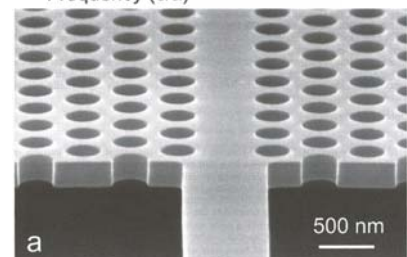
Present theory



Experiment of Ref. [1]



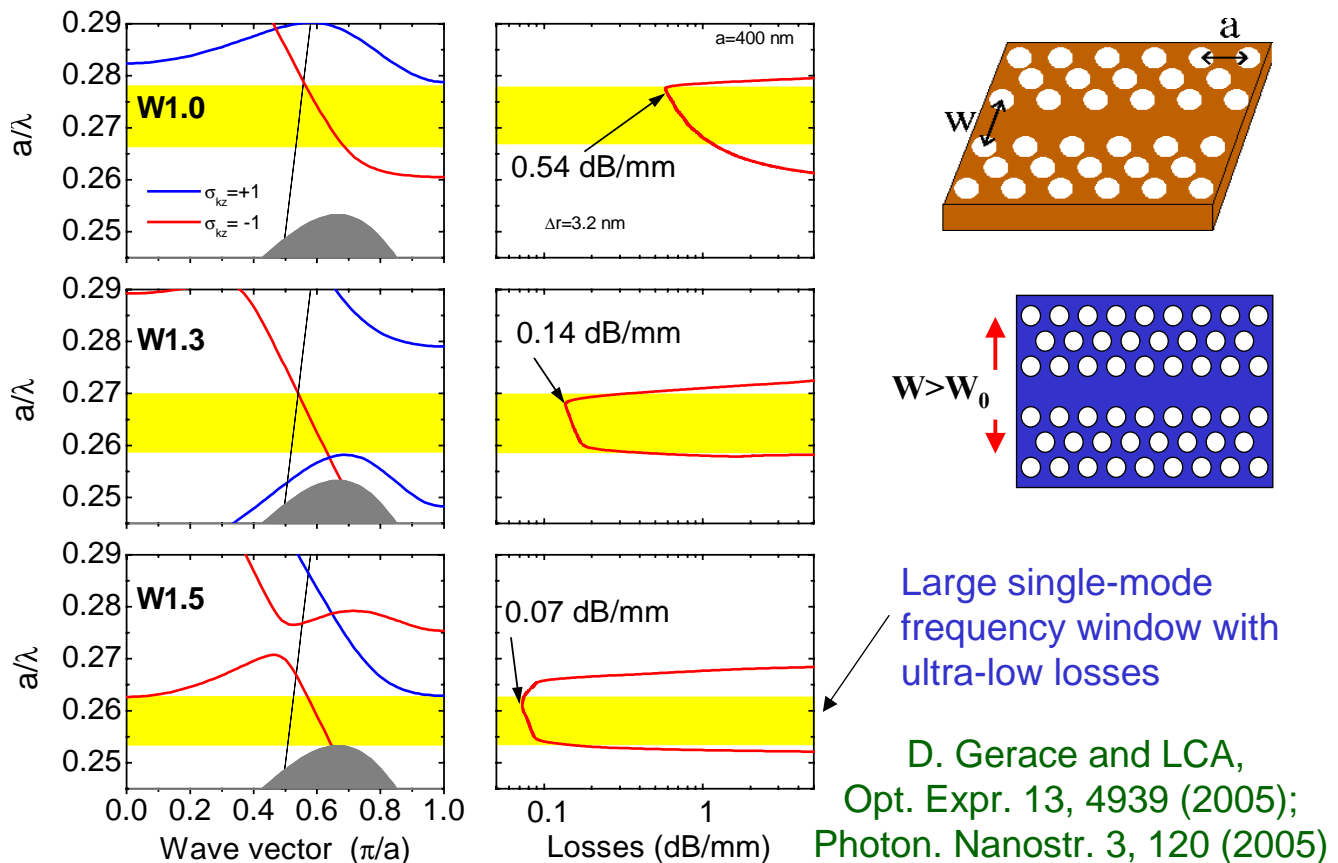
Theory with no fitting parameters



air bridge W1 waveguide,  $d/a=0.494$ ,  $r/a=0.37$ ,  $\Delta r=5$  nm,  $a=445$  nm

<sup>[1]</sup>S.J. McNab, N. Moll, Yu. Vlasov, Optics Express 11, 2923 (2003)

# Line-defects with increased channel width



## Conclusions

- The GME method is APPROXIMATE for both the photonic mode dispersion (as the basis set does not contain radiative modes of the effective waveguide) and for the losses (because radiative PhC modes are replaced with those of the effective waveguide).
- The results are close to those of “exact” methods in many common situation. The GME method is most reliable for high index-contrast PhC slabs (membranes, SOI) and for not too high air fractions.
- Main advantages: computational efficiency (especially in the case of low losses: high-Q nanocavities...) and physical insight when comparing with ideal 2D and homogeneous waveguide systems.
- Possible extensions (some underway):
  - Improve upon the approximations
  - PhC slabs with more than three layers
  - Radiation-matter interaction
  - Disorder-induced losses...

# Appendix: matrix elements etc.

## Basis set for guided-mode expansion

Let us denote by

$\mathbf{g} = g\hat{\mathbf{g}}$  the 2D wavevector in the xy plane with modulus  $g$

$\hat{\mathbf{e}}_{\mathbf{g}} = \hat{\mathbf{z}} \times \hat{\mathbf{g}}$  a unit vector perpendicular to both  $\hat{\mathbf{g}}$  and  $\hat{\mathbf{z}}$

$\omega_g$  the frequency of a guided mode

$$\chi_1 = \left( g^2 - \bar{\epsilon}_1 \frac{\omega_g^2}{c^2} \right)^{1/2}, \quad q = \left( \bar{\epsilon}_2 \frac{\omega_g^2}{c^2} - g^2 \right)^{1/2}, \quad \chi_3 = \left( g^2 - \bar{\epsilon}_1 \frac{\omega_g^2}{c^2} \right)^{1/2}$$

The guided modes frequencies of the effective waveguide are found from

$$q(\chi_1 + \chi_3)\cos(qd) + (\chi_1\chi_3 - q^2)\sin(qd) = 0, \quad \text{TE modes}$$

$$\frac{q}{\bar{\epsilon}_2} \left( \frac{\chi_1}{\bar{\epsilon}_1} + \frac{\chi_3}{\bar{\epsilon}_3} \right) \cos(qd) + \left( \frac{\chi_1}{\bar{\epsilon}_1} \frac{\chi_3}{\bar{\epsilon}_3} - \frac{q^2}{\bar{\epsilon}_2^2} \right) \sin(qd) = 0, \quad \text{TM modes}$$

## Guided mode profile: TE

$$\mathbf{E}_\mu^{\text{guided}}(\boldsymbol{\rho}, z) = \frac{e^{i\mathbf{g} \cdot \boldsymbol{\rho}}}{\sqrt{S}} i \frac{\omega_\mu}{c} \hat{\mathbf{e}}_g \begin{cases} A_{3\mu} e^{-\chi_{3\mu}(z-d/2)}, & z > \frac{d}{2} \\ A_{2\mu} e^{iq_\mu z} + B_{2\mu} e^{-iq_\mu z}, & |z| < \frac{d}{2} \\ B_{1\mu} e^{\chi_{1\mu}(z+d/2)}, & z < -\frac{d}{2} \end{cases} \quad (\text{A1})$$

$$\mathbf{H}_\mu^{\text{guided}}(\boldsymbol{\rho}, z) = \frac{e^{i\mathbf{g} \cdot \boldsymbol{\rho}}}{\sqrt{S}} \begin{cases} A_{3\mu}(\chi_{3\mu} \hat{g} + ig \hat{z}) e^{-\chi_{3\mu}(z-d/2)}, & z > \frac{d}{2} \\ A_{2\mu} i(-q_\mu \hat{g} + g \hat{z}) e^{iq_\mu z} + B_{2\mu} i(q_\mu \hat{g} + g \hat{z}) e^{-iq_\mu z}, & |z| < \frac{d}{2} \\ B_{1\mu}(-\chi_{1\mu} \hat{g} + ig \hat{z}) e^{\chi_{1\mu}(z+d/2)}, & z < -\frac{d}{2} \end{cases} \quad (\text{A2})$$

$$\begin{aligned} A_2 &= \frac{B_1}{2q} (q - i\chi_1) e^{iqd/2} \\ B_2 &= \frac{B_1}{2q} (q + i\chi_1) e^{-iqd/2} \\ A_3 &= \frac{B_1}{2q\chi_3} [q(\chi_3 - \chi_1) \cos(qd) + (q^2 + \chi_1\chi_3) \sin(qd)] \end{aligned}$$

$$\frac{\chi_1^2 + g^2}{2\chi_1} |B_1|^2 + \frac{\chi_3^2 + g^2}{2\chi_3} |A_3|^2 + d \left[ (g^2 + q^2)(|A_2|^2 + |B_2|^2) + (g^2 - q^2)(A_2^* B_2 + B_2^* A_2) \frac{\sin(qd)}{qd} \right] = 1$$

## Guided mode profile: TM

$$\mathbf{H}_\mu^{\text{guided}}(\boldsymbol{\rho}, z) = \frac{e^{i\mathbf{g} \cdot \boldsymbol{\rho}}}{\sqrt{S}} \hat{\mathbf{e}}_g \begin{cases} C_{3\mu} e^{-\chi_{3\mu}(z-d/2)}, & z > \frac{d}{2} \\ C_{2\mu} e^{iq_\mu z} + D_{2\mu} e^{-iq_\mu z}, & |z| < \frac{d}{2} \\ D_{1\mu} e^{\chi_{1\mu}(z+d/2)}, & z < -\frac{d}{2} \end{cases} \quad (\text{A7})$$

$$\mathbf{E}_\mu^{\text{guided}}(\boldsymbol{\rho}, z) = \frac{e^{i\mathbf{g} \cdot \boldsymbol{\rho}}}{\sqrt{S}} i \frac{c}{\omega_g} \begin{cases} \frac{1}{\bar{\epsilon}_3} C_{3\mu}(\chi_{3\mu} \hat{g} + ig \hat{z}) e^{-\chi_{3\mu}(z-d/2)}, & z > \frac{d}{2} \\ \frac{1}{\bar{\epsilon}_2} [C_{2\mu} i(-q_\mu \hat{g} + g \hat{z}) e^{iq_\mu z} + D_{2\mu} i(q_\mu \hat{g} + g \hat{z}) e^{-iq_\mu z}], & |z| < \frac{d}{2} \\ \frac{1}{\bar{\epsilon}_1} D_{1\mu}(-\chi_{1\mu} \hat{g} + ig \hat{z}) e^{\chi_{1\mu}(z+d/2)}, & z < -\frac{d}{2} \end{cases} \quad (\text{A8})$$

The appropriate relations between coefficients can be derived from (A3)-(A5) by the replacements  $A \rightarrow C$ ,  $B \rightarrow D$  and  $\chi_1 \rightarrow \chi_1/\bar{\epsilon}_1$ ,  $q \rightarrow q/\bar{\epsilon}_2$  (except in the trigonometric functions),  $\chi_3 \rightarrow \chi_3/\bar{\epsilon}_3$ . The normalization integral of the magnetic field gives the condition

$$\frac{|D_1|^2}{2\chi_1} + \frac{|C_3|^2}{2\chi_3} + d \left[ |C_2|^2 + |D_2|^2 + (C_2^* D_2 + D_2^* C_2) \frac{\sin(qd)}{qd} \right] = 1. \quad (\text{A9})$$



# Matrix elements between guided modes

$$\mathcal{H}_{\mu\nu}^{\text{TE-TE}} = \left(\frac{\omega_\mu}{c}\right)^2 \left(\frac{\omega_\nu}{c}\right)^2 \hat{\mathbf{e}}_{\mathbf{g}} \cdot \hat{\mathbf{e}}_{\mathbf{g}'} \left\{ (\bar{\epsilon}_1)^2 \eta_1(\mathbf{G}, \mathbf{G}') B_{1\mu}^* B_{1\nu} I_1 + (\bar{\epsilon}_3)^2 \eta_3(\mathbf{G}, \mathbf{G}') A_{3\mu}^* A_{3\nu} I_3 \right. \\ \left. + (\bar{\epsilon}_2)^2 \eta_2(\mathbf{G}, \mathbf{G}') [(A_{2\mu}^* A_{2\nu} + B_{2\mu}^* B_{2\nu}) I_{2-} + (A_{2\mu}^* B_{2\nu} + B_{2\mu}^* A_{2\nu}) I_{2+}] \right\},$$

$$\mathcal{H}_{\mu\nu}^{\text{TM-TM}} = \eta_1(\mathbf{G}, \mathbf{G}') D_{1\mu}^* D_{1\nu} (\chi_{1\mu} \chi_{1\nu} \hat{\mathbf{g}} \cdot \hat{\mathbf{g}}' + gg') I_1 + \eta_3(\mathbf{G}, \mathbf{G}') C_{3\mu}^* C_{3\nu} (\chi_{3\mu} \chi_{3\nu} \hat{\mathbf{g}} \cdot \hat{\mathbf{g}}' + gg') I_3 \\ + \eta_2(\mathbf{G}, \mathbf{G}') [(C_{2\mu}^* C_{2\nu} + D_{2\mu}^* D_{2\nu}) (q_\mu q_\nu \hat{\mathbf{g}} \cdot \hat{\mathbf{g}}' + gg') I_{2-} + (C_{2\mu}^* D_{2\nu} + D_{2\mu}^* C_{2\nu}) (-q_\mu q_\nu \hat{\mathbf{g}} \cdot \hat{\mathbf{g}}' + gg') I_{2+}],$$

$$\mathcal{H}_{\mu\nu}^{\text{TE-TM}} = \left(\frac{\omega_\mu}{c}\right)^2 \hat{\mathbf{e}}_{\mathbf{g}} \cdot \hat{\mathbf{g}}' \left\{ -\bar{\epsilon}_1 \eta_1(\mathbf{G}, \mathbf{G}') B_{1\mu}^* D_{1\nu} \chi_{1\nu} I_1 + \bar{\epsilon}_3 \eta_3(\mathbf{G}, \mathbf{G}') A_{3\mu}^* C_{3\nu} \chi_{3\nu} I_3 \right. \\ \left. + i\bar{\epsilon}_2 \eta_2(\mathbf{G}, \mathbf{G}') q_\nu [(-A_{2\mu}^* C_{2\nu} + B_{2\mu}^* D_{2\nu}) I_{2-} + (A_{2\mu}^* D_{2\nu} - B_{2\mu}^* C_{2\nu}) I_{2+}] \right\},$$

$$\mathcal{H}_{\mu\nu}^{\text{TM-TE}} = \left(\frac{\omega_\nu}{c}\right)^2 \hat{\mathbf{g}} \cdot \hat{\mathbf{e}}_{\mathbf{g}'} \left\{ -\bar{\epsilon}_1 \eta_1(\mathbf{G}, \mathbf{G}') D_{1\mu}^* B_{1\nu} \chi_{1\mu} I_1 + \bar{\epsilon}_3 \eta_3(\mathbf{G}, \mathbf{G}') C_{3\mu}^* A_{3\nu} \chi_{3\mu} I_3 \right. \\ \left. - i\bar{\epsilon}_2 \eta_2(\mathbf{G}, \mathbf{G}') q_\mu [(-C_{2\mu}^* A_{2\nu} + D_{2\mu}^* B_{2\nu}) I_{2-} + (D_{2\mu}^* A_{2\nu} - C_{2\mu}^* B_{2\nu}) I_{2+}] \right\}.$$

$$I_1 = (\chi_{1\mu} + \chi_{1\nu})^{-1}, \quad I_{2\pm} = \frac{\sin((q_\mu \pm q_\nu)d/2)}{(q_\mu \pm q_\nu)/2}, \quad I_3 = (\chi_{3\mu} + \chi_{3\nu})^{-1}$$

→ diel. tensor

## Radiative mode profiles

$$q_j = \left( \bar{\epsilon}_j \frac{\omega^2}{c^2} - g^2 \right)^{1/2}, \quad j = 1, 2, 3. \quad \hat{\mathbf{e}}_{\mathbf{g}} = \hat{\mathbf{z}} \times \hat{\mathbf{g}} \quad z_1 = -d/2, \quad z_2 = 0, \quad z_3 = d/2$$

**TE modes. Normalization:**  $W_1 = 0, X_1 = 1/\sqrt{\bar{\epsilon}_1}$  or  $W_3 = 1/\sqrt{\bar{\epsilon}_3}, X_3 = 0$ .

$$\mathbf{E}_j^{\text{rad}}(\boldsymbol{\rho}, z) = \frac{e^{i\mathbf{g} \cdot \boldsymbol{\rho}}}{\sqrt{S}} i \hat{\mathbf{e}}_{\mathbf{g}} [W_j e^{iq_j(z-z_j)} + X_j e^{-iq_j(z-z_j)}], \quad (\text{D2})$$

$$\mathbf{H}_j^{\text{rad}}(\boldsymbol{\rho}, z) = \frac{e^{i\mathbf{g} \cdot \boldsymbol{\rho}}}{\sqrt{S}} i \frac{c}{\omega} [(g\hat{\mathbf{z}} - q_j \hat{\mathbf{g}}) W_j e^{iq_j(z-z_j)} + (g\hat{\mathbf{z}} + q_j \hat{\mathbf{g}}) X_j e^{-iq_j(z-z_j)}]. \quad (\text{D3})$$

**TM modes. Normalization:**  $Y_1 = 0, Z_1 = 1$  or  $Y_3 = 1, Z_3 = 0$ .

$$\mathbf{H}_j^{\text{rad}}(\boldsymbol{\rho}, z) = \frac{e^{i\mathbf{g} \cdot \boldsymbol{\rho}}}{\sqrt{S}} \hat{\mathbf{e}}_{\mathbf{g}} [Y_j e^{iq_j(z-z_j)} + Z_j e^{-iq_j(z-z_j)}], \quad (\text{D6})$$

$$\mathbf{E}_j^{\text{rad}}(\boldsymbol{\rho}, z) = -\frac{e^{i\mathbf{g} \cdot \boldsymbol{\rho}}}{\sqrt{S}} \frac{c}{\bar{\epsilon}_j \omega} [(g\hat{\mathbf{z}} - q_j \hat{\mathbf{g}}) Y_j e^{iq_j(z-z_j)} + (g\hat{\mathbf{z}} + q_j \hat{\mathbf{g}}) Z_j e^{-iq_j(z-z_j)}]. \quad (\text{D7})$$

N.b. when  $q_j$  is imaginary, the mode does not contribute to losses.

# Matrix elements guided $\leftrightarrow$ radiative

$$\begin{aligned} \mathcal{H}_{\mu,r}^{\text{TE-TE}} &= \left( \frac{\omega_\mu}{c} \right)^2 \frac{\omega_r}{c} \hat{\epsilon}_{\mathbf{g}} \cdot \hat{\epsilon}_{\mathbf{g}'} \times \\ &\left\{ (\bar{\epsilon}_1)^2 \eta_1(\mathbf{G}, \mathbf{G}') B_{1\mu}^* (W_{1r} I_{1+} + X_{1r} I_{1-}) + (\bar{\epsilon}_3)^2 \eta_3(\mathbf{G}, \mathbf{G}') A_{3\mu}^* (W_{3r} I_{3-} + X_{3r} I_{3+}) \right. \\ &\left. + (\bar{\epsilon}_2)^2 \eta_2(\mathbf{G}, \mathbf{G}') [(A_{2\mu}^* W_{2r} + B_{2\mu}^* X_{2r}) I_{2-} + (A_{2\mu}^* X_{2r} + B_{2\mu}^* W_{2r}) I_{2+}] \right\}, \end{aligned} \quad (\text{E1})$$

$$\begin{aligned} \mathcal{H}_{\mu,r}^{\text{TM-TM}} &= \eta_1(\mathbf{G}, \mathbf{G}') D_{1\mu}^* [(gg' + i\chi_{1\mu} q_{1r} \hat{g} \cdot \hat{g}') Y_{1r} I_{1+} + (gg' - i\chi_{1\mu} q_{1r} \hat{g} \cdot \hat{g}') Z_{1r} I_{1-}] \\ &+ \eta_3(\mathbf{G}, \mathbf{G}') C_{3\mu}^* [(gg' - i\chi_{3\mu} q_{3r} \hat{g} \cdot \hat{g}') Y_{3r} I_{3-} + (gg' + i\chi_{3\mu} q_{3r} \hat{g} \cdot \hat{g}') Z_{3r} I_{3+}] \\ &+ \eta_2(\mathbf{G}, \mathbf{G}') [(C_{2\mu}^* Y_{2r} + D_{2\mu}^* Z_{2r})(gg' + q_\mu q_{2r} \hat{g} \cdot \hat{g}') I_{2-} + (C_{2\mu}^* Z_{2r} + D_{2\mu}^* Y_{2r})(gg' - q_\mu q_{2r} \hat{g} \cdot \hat{g}') I_{2+}], \end{aligned} \quad (\text{E2})$$

$$\begin{aligned} \mathcal{H}_{\mu,r}^{\text{TE-TM}} &= i \left( \frac{\omega_\mu}{c} \right)^2 \hat{\epsilon}_{\mathbf{g}} \cdot \hat{g}' \left\{ \bar{\epsilon}_1 \eta_1(\mathbf{G}, \mathbf{G}') q_{1r} B_{1\mu}^* (-Y_{1r} I_{1+} + Z_{1r} I_{1-}) + \bar{\epsilon}_3 \eta_3(\mathbf{G}, \mathbf{G}') q_{3r} A_{3\mu}^* (-Y_{3r} I_{3-} + Z_{3r} I_{3+}) \right. \\ &\left. + \bar{\epsilon}_2 \eta_2(\mathbf{G}, \mathbf{G}') q_{2r} [(-A_{2\mu}^* Y_{2r} + B_{2\mu}^* Z_{2r}) I_{2-} + (A_{2\mu}^* Z_{2r} - B_{2\mu}^* Y_{2r}) I_{2+}] \right\}, \end{aligned} \quad (\text{E3})$$

$$\begin{aligned} \mathcal{H}_{\mu,r}^{\text{TM-TE}} &= \frac{\omega_r}{c} \hat{g} \cdot \hat{\epsilon}_{\mathbf{g}'} \left\{ -\bar{\epsilon}_1 \eta_1(\mathbf{G}, \mathbf{G}') \chi_{1\mu} D_{1\mu}^* (W_{1r} I_{1+} + X_{1r} I_{1-}) + \bar{\epsilon}_3 \eta_3(\mathbf{G}, \mathbf{G}') \chi_{3\mu} C_{3\mu}^* (W_{3r} I_{3-} + X_{3r} I_{3+}) \right. \\ &\left. - i\bar{\epsilon}_2 \eta_2(\mathbf{G}, \mathbf{G}') q_\mu [(D_{2\mu}^* X_{2r} - C_{2\mu}^* W_{2r}) I_{2-} + (D_{2\mu}^* W_{2r} - C_{2\mu}^* X_{2r}) I_{2+}] \right\}. \end{aligned} \quad (\text{E4})$$

$$I_{3\pm} = (\chi_{3\mu} \pm iq_{3r})^{-1}, \quad I_{2\pm} = \frac{\sin((q_\mu \pm q_{2r})d/2)}{(q_\mu \pm q_{2r})/2}, \quad I_{1\pm} = (\chi_{1\mu} \pm iq_{1r})^{-1}.$$

$\rightarrow$  coupling